Nanoscale

REVIEW

View Article Online
View Journal | View Issue



Cite this: *Nanoscale*, 2025, **17**, 15068

# A review: metal and metal oxide nanoparticles for environmental applications

Zhihua Yang and Jiawei Shen *

Environmental pollution has become a major issue since chemical species from different sources (*e.g.*, textile industries, paper industries, dye industries, *etc.*) have been introduced into our living environment. If these chemical species are not properly treated, they will be highly toxic and hazardous to living organisms. Thus, it is important to remove the chemical species before discharge into the environment. Varieties of techniques, such as degradation, adsorption, photocatalysis, *etc.*, have been employed to remove the chemical species. In recent years, metal and metal oxide nanoparticles, which exhibit high degradation and adsorption performance, have been widely used in environmental treatment. Here we provide a detailed overview of the environmental applications of metal and metal oxide nanoparticles, particularly in water treatment. The metal and metal oxide nanoparticles possess immense potential in environmental applications, however, challenges such as agglomeration, toxicity concerns, and cost-effectiveness are acknowledged. Through a comprehensive analysis of existing literature, this review systematically integrates critical research data. And it presents relevant research findings, aiming to explore environmentally sustainable nanomaterials with superior contaminant removal efficiency and broad applicability.

Received 13th May 2025,
Accepted 30th May 2025

DOI: 10.1039/d5nr01973g

rsc.li/nanoscale



## 1. Introduction

Chemical species, such as dyes and heavy metals, and toxicity, mainly stemming from textile dyeing, printing, manufacturing, *etc.*, have become a significant global environmental concern.[1–4] These pollutants can seriously impact the ecological environment and public health when discharged into aquatic systems or the atmosphere without treatment.[5,6] The continued presence of pollutants in the environment will disrupt the balance of the ecosystem, harm organisms, and even pose a threat to human health. Hence, effective and enduring solutions to treat pollution are desirable.

Metal and metal oxide nanoparticles (NPs) are widely used in various fields, such as optics, electronics, thermodynamics, catalysis, *etc.*, since they possess unique characteristics.[7–10] As illustrated in Fig. 1, the number of publications focusing on the environmental applications of metal and metal oxide NPs has demonstrated a consistent annual increase. Notably, research articles and review articles constitute the predominant publication types, accounting for 96.14% of the total literature. Generally, NPs possess a high surface area and thus exhibit good adsorption performance, which renders them suitable for addressing environmental pollution.[6,11,12] In recent years, research has shown that the exceptional photocatalytic, degradation, and adsorption capabilities of the NPs have made them widely used in the removal of dyes, heavy metals, and toxic substances.[2,4,13–18] Therefore, metal and metal oxide NPs are a promising tool in the fight against environmental pollution.

In this review, we provide a detailed introduction to the environmental applications of metal and metal oxide NPs. We aim to delve into the physical–chemical properties, synthesis processes of the NPs, and the removal mechanism of the pollutants. Practical applications and research have confirmed the practicality of these NPs, but at the same time, some challenges have also arisen. Exploring metal and metal oxide NPs for environmental applications provides us a with better understanding of the removal process of the pollutants and holds the potential to offer new insights into leading-edge research.

Metal and metal oxide NPs facilitate environmental remediation through three primary mechanisms: adsorbents (see Table 1), catalysts (see Table 2), and sensors for hazardous substances (see Table 3). The tables systematically consolidate case studies of environmental remediation using metal and metal oxide NPs, categorized by type of pollutants and NPs and other critical parameters.

This review focuses on recent research progress regarding metal and metal oxide NPs in environmental applications. It systematically summarizes synthesis methods, key pollutant removal mechanisms, and critical influencing factors.[19]

*School of Physics, Hangzhou Normal University, Hangzhou 311121, P. R. China.*
*E-mail: jwshen@hznu.edu.cn*

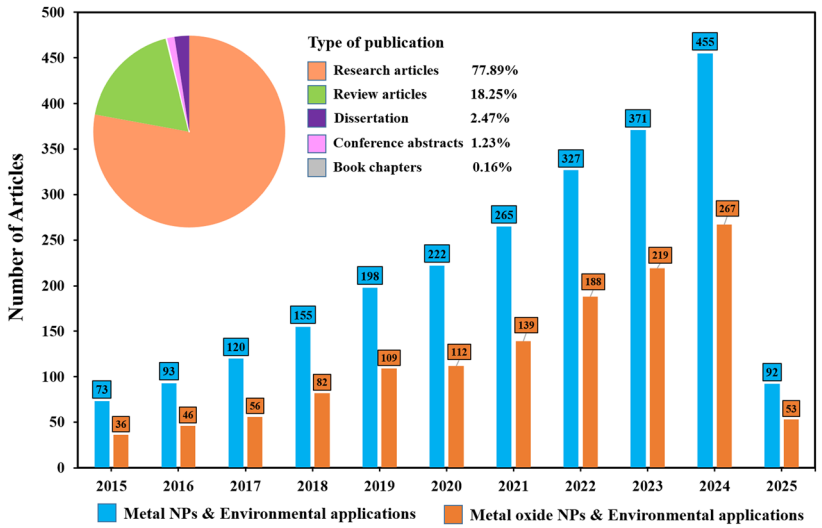


**Fig. 1** Statistics of articles published in the past 10 years on the topic "Metal NPs & environmental application", "Metal oxide NPs & environmental application", source: Web of Science (search performed in April 2025).

**Table 1** Metal and metal oxide nanoparticles adsorbents utilized for environmental remediation

| Type of pollutants | Type of NPs | Size (nm) | Morphology | Capacity (mg $g^{-1}$) | Ref. |
|---|---|---|---|---|---|
| Cd(II)/Pd(II)/Co(II)/ MB/Congo red | ZnO (using casein as biogenic agent) | 10 | Quasi-spherical | 156.74/194.93/67.93/ 115.47/62.19 | 4 |
| Cd(II) | $TiO_2$ (a sol–gel method) | 19.29–26.72 | Anatase phase | 29.28 | 18 |
| Cr(III)/Cr(VI) | Fe (nZVI in borohydride reduction) | 1–2 | Necklace-like | 453.5/372 | 93 |
| Cr(VI) | Fe (using leaves extracts) | 20–80 | Spherical | 34 | 83 |
| Cu(II) | $Fe_3O_4$ (chemical method) | 20–50 | Spherical | 28.12 | 169 |
| Divalent metallic ions | MgO (using bio-compatible acacia gum) | 40–78 | Flower shaped | | 134 |
| Phosphate | MgO (using PSS as agent) | 2–250 | Spherical/nanoflakes | 75.13 | 146 |
| Tetracycline | $ZrO_2$ (using plant extracts) | 5.9–8.5 | Spherical | 30.45 | 17 |
| Tetracycline | $ZrO_2$ (using leaves extracts) | 15 | Spherical | 526.32 | 161 |
| Congo red | MgO (chemical method) | 500 | Microrods | 160 | 137 |
| MB/cresol red | $Fe_3O_4$ (chemical method) | 250 | Spherical | 44.38/11.22 | 168 |
| MB | $ZrO_2$ (using pericarp extracts) | 10 | Spherical | 23.26 | 155 |
| MB | Ag (loaded on activated carbon) | 15–80 | Semi-spherical | 71.4 | 44 |
| Cocktail dye | Ag (protein mediated) | 10 ± 2.5 | Spherical | 547.5 | 45 |
| Fluoride | $Fe_3O_4$ (using jojoba defatted meal) | 51.48 | Spherical and rectangular | 34.48 | 170 |
| Fluoride | $TiO_2$ (biological method) | 24.33–91.49 | Anatase, anatase mix rutile and rutile phase | 0.85 | 183 |
| Bioaerosols | Ag (loaded on activated carbon) | 12–16 | Spherical | Complete inhibition | 38 |

**Table 2** Metal and metal oxide nanoparticles catalysts utilized for environmental remediation

| Type of pollutants | Type of NPs | Size (nm) | Morphology | Capacity (mg $g^{-1}$) | Ref. |
|---|---|---|---|---|---|
| Azo dyes | Ag (bacterial method) | 11.2–39.0 | Spherical | 541.4–969.2 | 14 |
| MB | Au (loaded on surface of Hap) | 2–6 | Elongated | 522 | 58 |
| MCB | Fe (using tea extracts) | 20–40 | Spherical | 67.5 | 82 |
| MO | Fe (using leaves extracts) | 43–220 | Spherical | 900 | 84 |
| MB/MO | ZnO (using leaves extracts) | 10–16 | Spherical | 430/422 | 16 |
| MB | $TiO_2$ (chemical method) | 135–155 | Cup-like/spherical | | 181 |
| MB/MO | $TiO_2$ (chemical method) | 91–103 | Hollow spherical | | 182 |

Furthermore, the review presents the size and morphological characteristics of NPs prepared *via* different methods, providing valuable insights for researchers in nanoparticle fabrication.[20] Additionally, it discusses current research trends, challenges, and future perspectives on the use of metal and metal oxide NPs in environmental remediation.[21]

Table 3 Metal nanoparticles sensors utilized for environmental remediation

| Type of pollutants | Type of NPs | Size (nm) | Morphology | Detection limit | Ref. |
|---|---|---|---|---|---|
| $Pb^{2+}$ | Au (capped with NDTM) | 29 ± 7 | Spherical | 0.35μmol $L^{-1}$ | 62 |
| $NO_2$ gas | Cu (functionalized with RGO) | 7–29 | Spherical | 100 ppm | 96 |
| *p*-NT | Cu (using chemical method) | 5 | Cluster | 0.1 μmol $L^{-1}$ | 100 |

# 2. Metal nanoparticles

## 2.1 Noble metal nanoparticles

Noble metals include silver (Ag), gold (Au), platinum (Pt), rhodium (Rh), ruthenium (Ru), palladium (Pd), and so on.[22] Among all noble metals, Au and Ag NPs are most extensively studied due to the well-established synthesis routes, their relatively higher content in the Earth's crust, and better safety profile.[23–25] Noble metal NPs in optics, electronics, thermodynamics, and catalysis with unusual performance are widely used in various fields.[9,10,26–30]

**2.1.1 Silver nanoparticles.** Silver nanoparticles (Ag NPs), due to their unique properties,[13,31,32] are considered some of the most effective materials in environmental areas.[11,33,34] A major function of Ag NPs is as a fungicide, attributed to the antibacterial properties of silver. Research demonstrates the biocidal activity of Ag NPs against Gram-negative bacteria, viruses, and fungi.[35–37] Its antibacterial properties can be used to exploit for air and water disinfection. In addition, Ag NPs can also be used to remove some harmful gases from the environment by reacting with them.[38]

The general mechanism of removing contaminants from water with Ag NPs includes adsorption and photocatalytic degradation.[31] Photocatalysis is the main mechanism of dye wastewater treatment, wherein electrons are excited from the valence band to the conduction band upon irradiation, resulting in electron–hole pairs (Fig. 2b).[39] These electron–hole pairs undergo redox reactions with water and oxygen, leading to the formation of hydroxyl radical (–OH) and an anion radical ($–O_2^-$).[40] The hydroxyl radical acts as a strong oxidant and completely degrades the dye to a harmless product ($CO_2$, $H_2O$, *etc.*) (Fig. 2a).[13]

The biological methods of Ag NPs synthesis using biological entities like bacteria, yeast, fungi, and plants were reported to be clean, nontoxic, cost-effective, and environmentally acceptable.[41–43] Temoor Ahmed *et al.*[14] prepared Ag NPs using the bacterial strain *Bacillus marisflavi* TEZ7. It can be found that the Ag NPs are helpful in the degradation of textile dyes and harmful effluents. More specifically, the photocatalytic degradation efficiency of biogenic Ag NPs for three azo dyes (such as direct blue-1, methyl red, and reactive black-5) is relatively high. Moreover, it is proven that the degradation intermediates are non-toxic to rice plants. Therefore, using these Ag NPs to treat textile dyes and harmful effluents is efficient, and the process is environmentally friendly.

The adsorption capacity of Ag NPs was confirmed by several studies. The study assessed the usability of Ag NPs loaded on activated carbon for the removal of methylene blue (MB) molecules from aqueous solutions.[44] And the results showed the maximum adsorption of 71.4 mg $g^{-1}$ for the adsorbent. In another study, the Ag NPs fabricated with nano-silica powders were applied to adsorb dyes such as Congo red, Eosin yellow.[45] The results showed 99% removal of dyes at an initial concentration of 50 mg $L^{-1}$. Moreover, a novel composite of Ag NPs with polymers was reported to have efficient adsorption of MB and its catalytic reduction.[46]

Another way to use the valuable properties of Ag NPs is the elimination of microbiological contamination of the air.[29] Activated carbon filters (ACF) containing Ag NPs were prepared through an electroless deposition method.[38] It is used in heating, ventilating, and air-conditioning (HVAC) to filter outdoor air and suppress microbial activity attached to the filter. The antimicrobial ACF filters can remove bioaerosols, including viruses, bacteria, fungi, and all varieties of living materials, so as to achieve the effect of purifying the air. Filtration and antibacterial tests of the filters were performed in an experimental setup designed for filtration tests, as shown in Fig. 3. Bioaerosols were measured by using an aerodynamic particle sizer (APS) upstream and downstream of the test filter. Results proved that silver-coated ACF filters were effective in cleaning the air and reducing the harm of microorganisms in the living environment.

The unique properties of Ag NPs have attracted the attention of many industries, especially those with a particular need for bactericidal effects.[25,28] Moreover, the shape of Ag NPs as well as the detailed exploration of adsorption kinetics of Ag NPs onto different biological macromolecules need to be further investigated to improve the performance of Ag NPs.[13,47]

**2.1.2 Gold nanoparticles.** Gold nanoparticles (Au NPs) have properties like photocatalytic performance,[48] efficient adsorption capacity,[49] and environmental friendliness,[50] *etc.* These properties make it show broad prospects in photocatalytic degradation, clean energy, and gas sensors.[51–53] With the further development of technology and the deepening of material research, the application of Au NPs in the field of environmental protection will be more extensive and in-depth.[54–56]

Surface plasmon resonance (SPR) is a crucial optical phenomenon possessed by plasmonic Au NPs. This phenomenon is produced by electromagnetic radiation, in which the free electrons of the metal surface are excited. In the visible region of the solar spectrum, the excitation results in the collective oscillation of surface electrons in Au NPs. Due to their plasmonic properties, they can effectively absorb sunlight, thereby improving the photocatalytic performance of the nano-

 

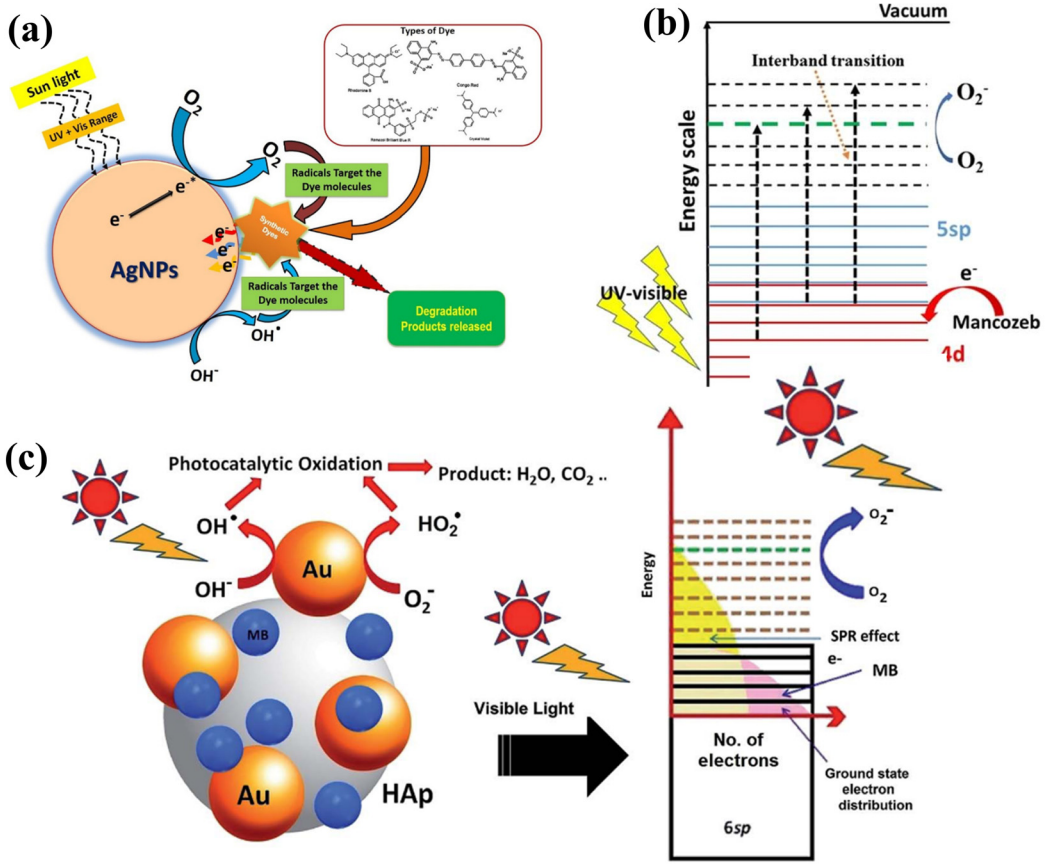


Fig. 2 (a) Schematic diagram of photocatalytic degradation dyes.[13] (b) Band structure of Ag NPs and its photocatalytic mechanism.[39] (c) Mechanism of waste removal utilizing plasmonic Au NPs based photocatalysts.[58] Reproduced from ref. 58 with permission from the Royal Society of Chemistry. Copyright © 2020 Elsevier B.V. All rights reserved.

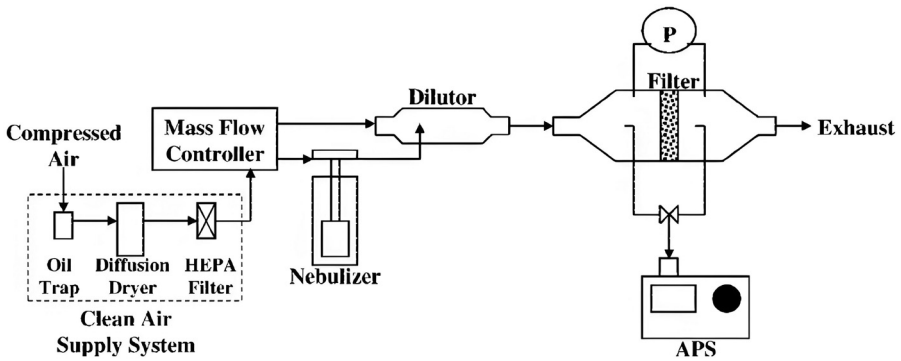


Fig. 3 Schematic diagram of experimental setup for the filtration tests.[38] Copyright © 2008, American Chemical Society.

material.[57] Therefore, if the nanomaterial containing Au NPs is used in wastewater treatment, these photoelectric properties can accelerate the photocatalytic oxidation reaction, and the process of removing pollutants from wastewater is done more efficiently.

Sudip Mondal *et al.*[58] reported a hydrothermally synthesized Au-loaded hydroxyapatite (HAp) NPs with mesoporous structures and a large surface area. The Au NPs were incorporated in different concentrations at the surface of HAp NPs, which seem to act as initializer and mediator of electron transfer for the oxidation reactions. In the visible range of solar light, the HAp supported Au NPs are involved in the photocatalytic oxidation, and the product is $H_2O$, $CO_2$, *etc.*, as shown in Fig. 2c. The experiment shows that the modeled MB removal efficiency will get a significant increase when treated by Au-loaded HAp NPs under visible light illumination (up to

32.47% in 9 h). Therefore, it is effective for the decomposition and removal of MB in a specially designed photocatalytic reactor containing Au NPs.

On the other hand, Au NPs based chemosensors have been developed for the colorimetric detection of heavy metals.[3,59] Moreover, Au NPs can be conjugated with other compounds to provide better stability, functionality, and biocompatibility.[60,61]

The research shows that rapid colorimetric sensing of $Pb^{2+}$ ions in water samples induces the aggregation of *N*-decanoyltromethamine (NDTM) loaded Au NPs, as shown in Fig. 4.[62] The color change from pink to violet in the presence of $Pb^{2+}$ is caused by the aggregation state of NDTM-Au NPs, and in this process, the average size of the NDTM-Au NPs increases from 34.5 nm to 57.5 nm measured by particle size analyzer.

Au NPs are actively employed in environmental applications, and they can be one of the potential applications for novel environmental applications. The performance of Au NPs is mainly controlled by the coating, size, and shape, and all these factors depend on the synthesis method and conditions such as time, temperature, pressure, PH, *etc*.[20,30] Therefore, in the future, good control of the reaction parameters will provide a way to improve the advantages of the potential applications of Au NPs.[23,24,63,64]

### 2.2 Transition metal nanoparticles

Transition metals refer to a series of metal elements in the d region of the periodic table, including Fe, Co, Ni, Cu, Mn, *etc*. Transition metals of different shapes and structures have been synthesized by various techniques since the 1960s.[65–67] These metal NPs exhibit excellent catalytic, optical, and electronic properties compared to bulk materials.[68–70] At present, the superior performance of Fe and Cu NPs is widely used in environmental remediation.

**2.2.1 Iron nanoparticles.** In the past decades, iron and iron-based NPs have aroused researchers' great interest due to their wide range of applications, such as environmental,[71] biomedical,[72] textiles,[73] healthcare,[74] food industry,[75] electronics,[76] renewable energies,[77] *etc*. So far, an increasing number of iron NPs, including green synthesized iron nanoparticles (Fe NPs),[78] nanoscale zero valent iron nanoparticles (nZVI),[79] and iron containing core–shell nanoparticles (CSNs)[80] have been fabricated for environmental applications. Generally, heavy metals like plumbum (Pb), chromium (Cr), and toxic dyes are released from industries into the environment.[81] Using iron and iron-based NPs is a useful way to improve the environment, since these NPs can effectively remove the heavy metals, chlorinated organic compounds, dyes, *etc*.[15]

*Green synthesized iron nanoparticles.* Green synthesis methods are generally accepted because of their non-toxic and low-cost characteristics. Kuang *et al.*[82] synthesized Fe NPs using tea extracts for the degradation of monochlorobenzene (MCB). It was found that Fe NPs synthesized by green tea extract have a degradation efficiency of 69% because of the existence of polyphenols/caffeine in the tea extract. Fe NPs prepared by *Eichhornia crassipes* leaf extracts show good performance of Cr removal (Fig. 5a), and the efficiency reached 89.9%, which is higher than Fe NPs synthesized by other methods.[83] Harshiny *et al.*[84] synthesized spherical Fe NPs from *Amaranthus dubius* leaf extract, which is a cubic phase structure with a diameter ranging from 43 to 220 nm (Fig. 5b). During the synthesis process, BFeNPs were prepared using a $NaBH_4$ solution, whereas DFeNPs were synthesized without this reagent. The process of synthesizing Fe NPs did not produce any other toxic by-products. The results show that it had a Methyl Orange (MO) degradation efficiency of 81% (Fig. 5c). Therefore, the green synthesis method of Fe NPs is feasible in environmental applications.

*Nanoscale zero valent iron nanoparticles.* The application of nZVI particles in the environment has significant potential and wide application prospects, especially in groundwater remediation,[85] soil pollution control,[86] and pollutant degradation,[87] *etc*. By injecting a suspension containing nZVI into formations, these NPs migrate in groundwater and induce redox reactions,[88] which can react with contaminants to remove them. In addition, because of its small particle size, the nZVI can be injected deep into formations where microbes cannot degrade to remediation the environment.[89] The technology is cost-effective and considered more environmentally

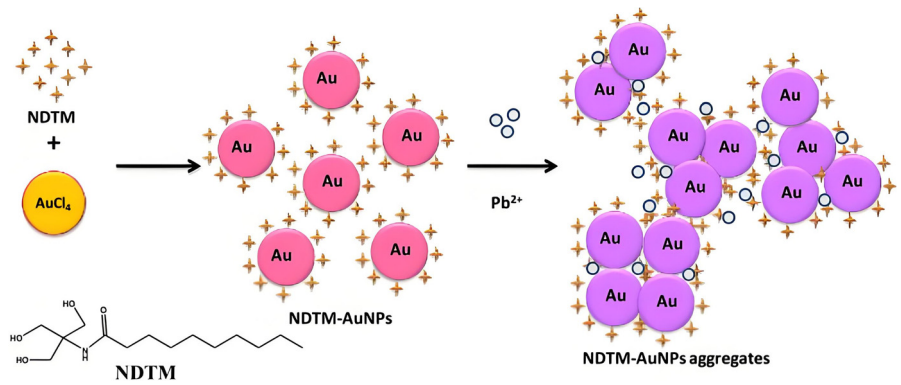


Fig. 4 Structure of NDTM and schematic representation of $Pb^{2+}$ sensing by NDTM-AuNPs.[62] Copyright © 2020 Elsevier B.V. All rights reserved.

 

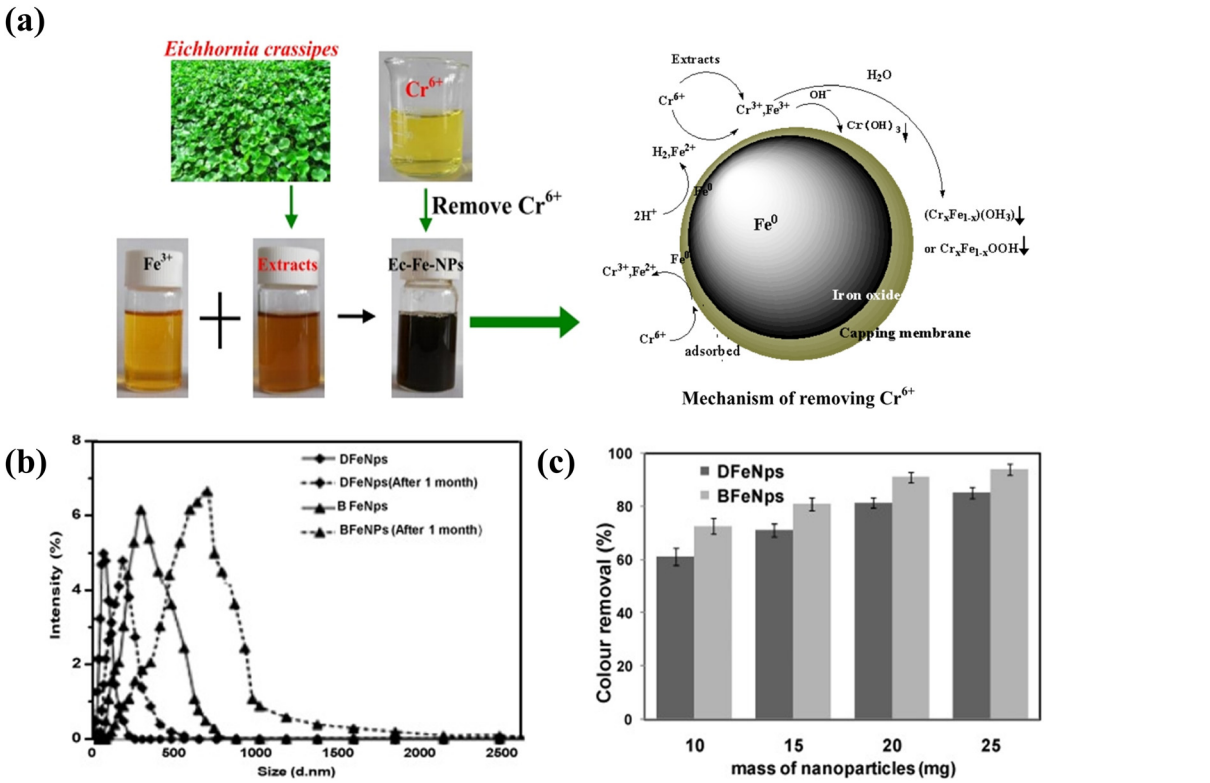


**Fig. 5** (a) The schematic diagram of Ec-Fe-NPs synthesized from *Eichhornia crassipes* leaf extracts and removal mechanism of Cr(VI).[83] (b) Size distributions of synthesised DFe Nps and BFe Nps. (c) The effect of Fe NPs mass on the color removal of MO dye.[84] 

friendly than traditional methods. This method has been successfully applied to the degradation of many pollutants, such as chlorinated organic compounds,[90] Cr,[91] and so on. What's more, the nZVI particles perform well in the reduction process, reacting with dissolved oxygen (DO), sulfates ($SO_4^{2+}$), nitrates ($NO_3^-$), *etc*.[92]

On the other hand, a synthesis method of resin-supported nanoscale zero-valent iron (R-nZVI) was reported.[93] The SEM images of resin without and with nZVI are shown in Fig. 6a and b, respectively. $Fe^{2+}$ undergoes the process of ion exchanged with resin, then reacts with $BH_4^-$ to form R-nZVI (Fig. 6c). R-nZVI can simultaneously remove chromium ions, including Cr(VI) and Cr(III). Moreover, the removal mechanisms of Cr(VI) and Cr(III) are different. At optimum conditions, the Cr(VI) removal efficiency was 84.4% when the initial concentration of Cr(VI) was 20.0 mg $L^{-1}$.

Furthermore, the nZVI can effectively remove As(V) from water without prior oxidative treatment or the use of additional chemicals.[2] The adsorption takes place at quite high efficiencies in a short time. The concentration of As(V) fell from 10 to 2.3 mg $L^{-1}$ after 60 min of contact, as shown in Fig. 7a. After the treatment with the nZVI, 77% As(V) removal was achieved. In later biological experiments, no lethal effects were observed. The nZVI-treated group exhibited significantly enhanced survival rates of *Rhinella arenarum* larvae compared to the control (Fig. 7b).

In the future, more detailed studies need to be performed, providing a clear description of the biomolecules and their role in mediating NPs synthesis. The aim is to influence the synthesis rate and improve the stability of the NPs.[94] Another development direction is the environmental remediation technology based on nZVI, since it is a valuable and novel technology. However, it is important to understand how nZVI particles interact with cells, so that the toxicity of nZVI can be reduced. Besides, we also need to find a cost-effective and large-scale production.[89]

**2.2.2 Copper nanoparticles.** The applications of copper nanoparticles (Cu NPs), which possess some interesting physical and chemical properties,[95] have generated a great deal of attention.[96–99] Because Cu is a 3d transition metal and it has a wide range of accessible oxidation states (Cu(0), Cu(I), Cu(II), and Cu(III)), Cu-based nanomaterials can promote a variety of reactions *via* both one- and two-electron pathways. In recent years, researchers have focused on sustainable approaches for environmentally friendly catalytic processes to detect chemical species.[98,100,101]

Volatile organic compounds (VOCs), such as ammonia, hydrogen sulfide, hydrogen peroxide, are harmful to the environment.[101,102] By monitoring level of VOCs, it can be confirmed that industrial production complies with safety regulations and that living things are not exposed to dangerous environment. Generally, Cu NPs have been used as a sensor

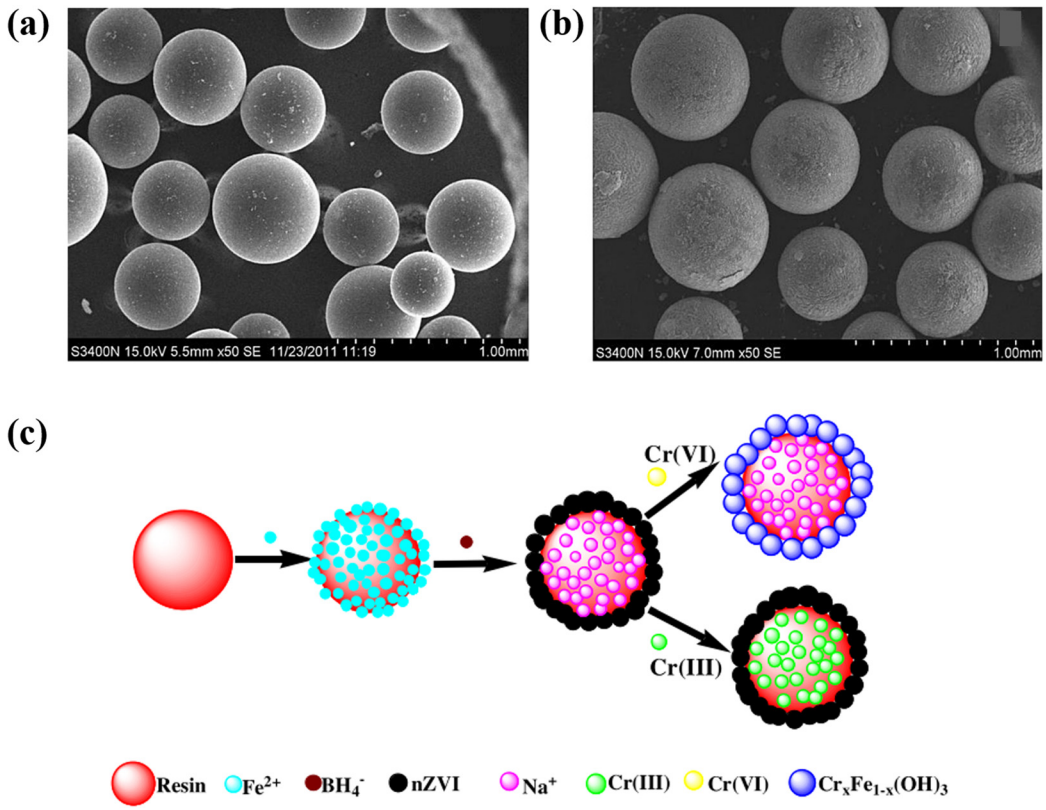


**Fig. 6** (a) SEM images of resin without nZVI. (b) SEM images of resin with nZVI (c) Schematic of Cr(VI) and Cr(III) removal mechanism by R-nZVI.[93] Crown Copyright © 2013 Published by Elsevier Ltd. All rights reserved.

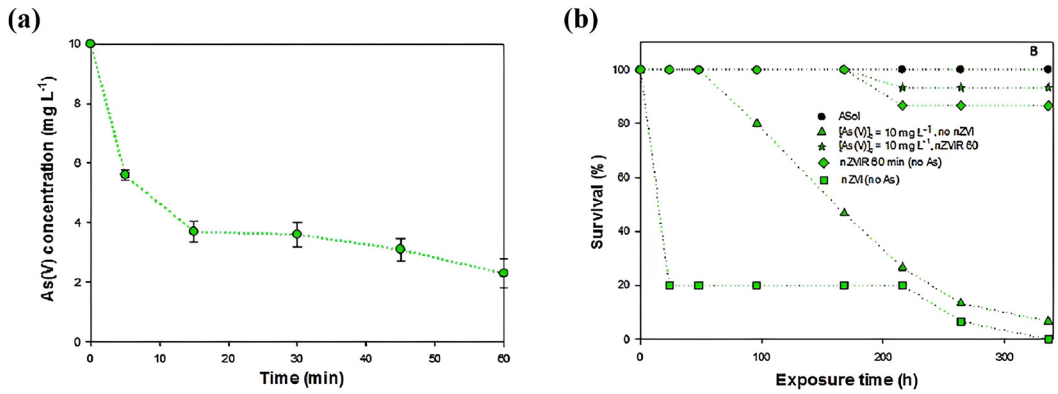


**Fig. 7** (a) Time profile of As(v) concentration during the treatment with nZVI. (b) Survival curves for *Rhinella arenarum* larvae under continuous 336-hour exposure to As(v) at varying nZVI concentrations.[2] Copyright © 2018 Elsevier B.V. All rights reserved.

for VOCs for several years and have proven to be a reliable method in VOCs' detection. For example, gas sensors based on reduced graphene oxides (RGOs) and Cu NPs have been prepared, which can be used to detect the $NO_2$ gas.[96]

The *p*-nitrotoluene (*p*-NT), as an intermediate in chemical dye, leads to water pollution and eventually threatens human health through the circulation of the ecosystem.[103] Long Chen *et al.*[100] designed a photoelectrochemical sensor composed of graphite carbon nitride nanosheets (CNNS) loaded Cu NPs, which can be applied for *p*-NT monitoring. In the paper, the mass ratio of the amount of copper added to the amount of CNNS is 2%, and the resulting product was labeled as CNNS-Cu 2%. After the redox reaction, *p*-NT species are reduced by receiving the electrons captured *via* the Cu(II) NPs, as shown in Fig. 8. In the process, the redox of Cu(II)/Cu(I) achieves a dynamic equilibrium.[104] The continuous consumption and rapid migration of photo-excited electron–hole pairs result in an enhanced photocurrent response, which facilitates sensitive *p*-NT detection. The photoelectric sensor can be used in the chemical and pharmaceutical fields and provides a

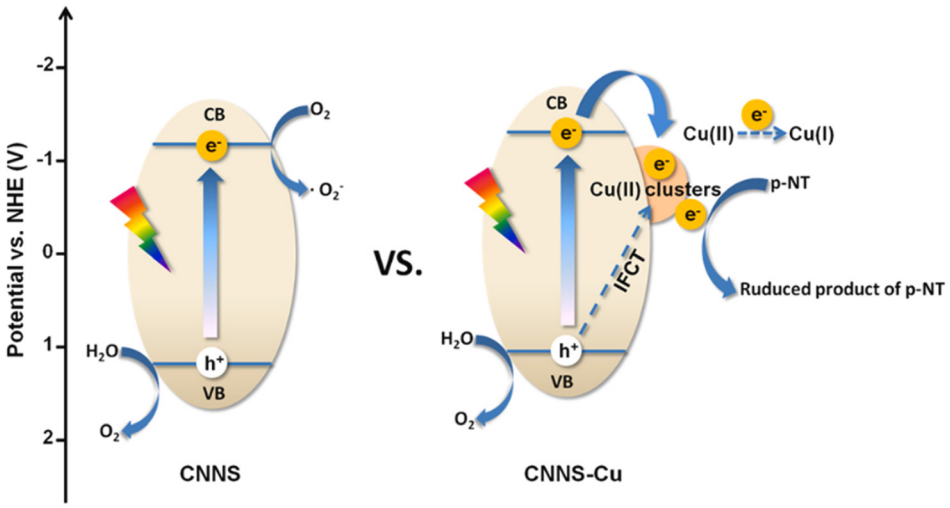


Fig. 8 The detection mechanism of *p*-NT based on CNNS-Cu 2%.[100] 

reference for the development of environmental detection in the future.[105,106] More efficient and durable materials need to be discovered, which is of great importance to the protection of the environment and human health.

Cu NPs have attracted a lot of attention because of their high performance and low cost. In the future, various synthesis methods will make it possible to control the size, shape, and morphology of NPs. This is useful for the design and development of Cu NPs with specific properties, such as electrocatalysis, photocatalysis, *etc*.[97,107,108]

Generally, metal NPs are synthesized through three different kinds of methods: physical, chemical, and biological (green). The size and shape of NPs strongly depend on various experimental parameters such as reaction time, pH, temperature, and so on.[109,110] Metal NPs primarily remove heavy metals through adsorption mechanisms. The biosynthesized metal NPs offer distinct advantages of being environmentally benign and non-toxic.[111] However, their removal capacity still requires improvement compared to chemically synthesized counterparts. For instance, Fe NPs (nZVI prepared *via* borohydride reduction) and Fe NPs (synthesized using plant leaf extracts) demonstrate Cr (VI) removal capacities of 372 mg $g^{-1}$ and 34 mg $g^{-1}$, respectively. On the other hand, these NPs effectively degrade dyes through catalytic processes. Notably, Ag NPs (produced *via* bacterial synthesis) exhibit an exceptional catalytic degradation capacity of 969.2 mg $g^{-1}$ for azo dyes. Additionally, they serve as effective detectors for hazardous substances, as exemplified by Au NPs (capped with NDTM) and Cu NPs (functionalized with RGO or synthesized by chemical method).

# 3. Metal oxide nanoparticles

Metal oxide nanoparticles, including titanium dioxide ($TiO_2$), zinc oxide (ZnO), iron oxide ($Fe_3O_4$), copper oxide (CuO), magnesium oxide (MgO), cerium oxide ($CeO_2$), *etc*., possess good characteristics (high surface area, good stability, and durability).[112–117] These metal oxide NPs are widely used in water treatment,[6] electrochemical environmental monitoring,[12] bio-nanotechnology,[118] *etc*. Through mechanisms like photocatalytic degradation and adsorption, these NPs efficiently break down complex dye molecules into simpler, less harmful byproducts. However, apparent problems of using metal oxide NPs need to be addressed properly, such as the aggregation of NPs, toxicity problems, and cost-effectiveness.[119]

## 3.1 Zinc oxide nanoparticles

Zinc oxide (ZnO) is a semiconductor material with a direct wide-band gap (about 3.3 eV)[120] and has high chemical and thermal stability.[121] These characteristics make ZnO stable at ambient conditions and hard to degrade. In the realm of the environment, ZnO nanoparticles (ZnO NPs) play a pivotal role in wastewater treatment, gas sensors, and ultraviolet (UV) detectors, because of their exceptional photocatalytic activity, good electrical conductivity, and optical transparency.[122,123]

Wastewater, which contains a significant number of organic pollutants such as textile dyes, pesticides, and pharmaceutical waste, should be treated before being discharged into the environment.[124] The ZnO NPs show excellent performance in the catalytic degradation of organic pollutants.[125] They can act as catalysts to promote the degradation of organic pollutants, thereby improving water quality.[126] In addition, they are able to effectively remove heavy metal ions in wastewater, because of their high specific surface area and good adsorption properties.[127–129]

Siripireddy Balaji *et al.*[16] carried out spherical ZnO NPs mediated by *Eucalyptus globulus* leaves extract under ambient conditions. TEM analysis revealed spherical nanoparticles with an average diameter of 11.6 nm (Fig. 9a). The ZnO NPs exhibit efficient photocatalytic activity in degrading MB and MO dyes (Fig. 9c and d). When ZnO NPs are illuminated under UV light, they produce electron–hole pairs. Further, these electron–hole pairs undergo redox reactions with water and

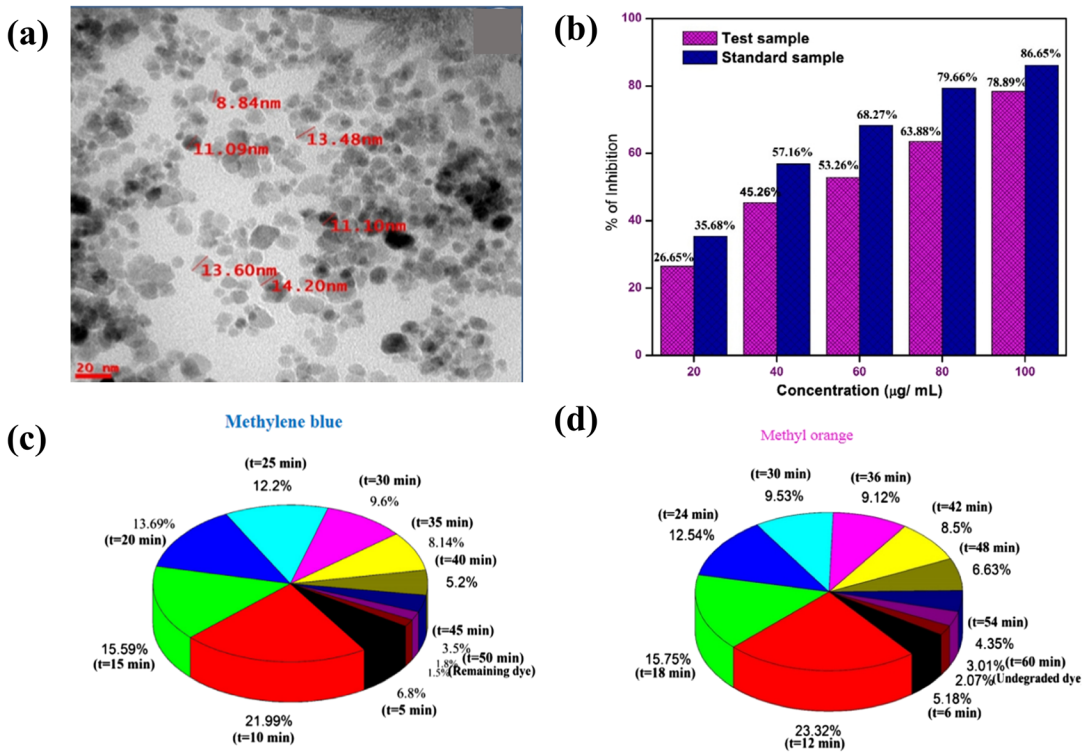


**Fig. 9** (a) TEM images of ZnO NPs at 20 nm. (b) Antioxidant activity of ZnO NPs by DPPH scavenging assay. Time-dependent photodegradation profiles (% of photodegradation *vs.* time) of (c) methylene blue and (d) methyl orange, presented as pie charts.[16] Copyright © 2016 The Society of Powder Technology Japan. Published by Elsevier B.V. and The Society of Powder Technology Japan. All rights reserved.

oxygen, leading to the formation of –OH and $-O_2^-$.[40] The MB and MO are degraded and the end product is $CO_2^+$ and $NO_3^-$. Synthesized ZnO NPs also exhibit high antioxidant activity against DPPH (1,1-diphenyl-2-picryl hydrazyl) molecule, in the antioxidant activity experiments (Fig. 9b). Moreover, the ZnO NPs synthesized from *Cassia fistula* leaves perform well in photodegradation of MB with an efficiency of 96.26–98.71% in the pH range of 2–4.[130]

Casein based biogenic-synthesis of ZnO NPs can be used to simultaneously decontaminate heavy metals, dyes, and pathogenic microbes from wastewater.[4] Casein as a capping agent contributed a highly negative charge to the surface of ZnO NPs, which enhanced the adsorption efficiency of cationic metals. The cationic metals, including divalent cadmium, cobalt, and plumbum ions [Cd(II), Co(II) and Pb(II)] were prepared by dissolving the required amounts of salts in Milli Q water. The metals, dyes, and microbes were adsorbed on the ZnO NPs surface (Fig. 10). After the adsorption, dyes were photo-degraded under UV irradiation. The ZnO NPs show maximum adsorption efficiency of 85.63% and 71.23% for Cd

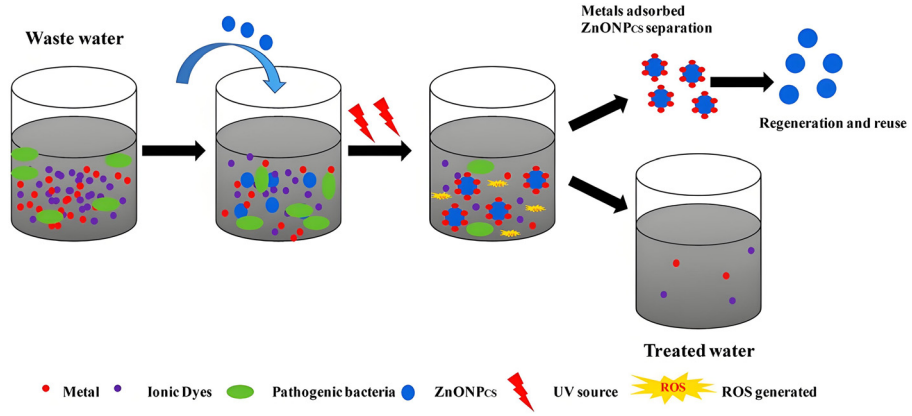


**Fig. 10** Schematic representation of how ZnO NPs can be used for systematic decontamination of wastewater containing metals, dyes, and microbes.[4] Copyright © 2018 Society of Chemical Industry.

 

(II) and Co(II), and 95.35% for Pb(II) at pH of 8.0. Furthermore, the ZnO NPs possess antibacterial properties and can inhibit the growth of bacteria vis ROS mediated oxidative stress.[131] The ZnO NPs used in the experiments were eventually recycled for reuse, which could be an economically promising strategy for wastewater treatment.

It is confirmed that ZnO NPs exhibit deleterious effects within aquatic ecosystems.[132] Notably, research has demonstrated that plants exhibit a certain degree of tolerance to ZnO NPs. However, when soil concentrations exceed 800 mg $kg^{-1}$, prolonged exposure may adversely affect plant defense systems, particularly antioxidant enzymes, ultimately inducing phytotoxicity.[133] Although ZnO NPs have many advantages, further research is needed to solve the biological toxicity problem before large-scale application.

### 3.2 Magnesium oxide nanoparticles

The properties of magnesium oxide nanoparticles (MgO NPs), such as biocompatible, excellent adsorption, low heat capacity, high melting point, and highly stable nature,[117,134–136] make it a suitable candidate for use in a wide range of applications.[136–139] The MgO NPs can be prepared through different chemical, physical, and biological routes, such as sol–gel,[140] hydrothermal,[141] vapor deposition method,[142] and plasma irradiation.[143] In general, these techniques require high energy and robust equipment to obtain MgO NPs. Therefore, biological (green) synthesis is the best substitute, because of its simple, economical, and environmentally friendly processing strategy.

Because of their excellent adsorption, the MgO NPs were used to adsorb dyes, heavy metals, and other pollutants in wastewater.[138,144] In order to improve the adsorption capacity, the synthesized MgO NPs surface area should be larger. Wang *et al.*[137] obtained the unique porous nanosheet-assembled structure of PS-MgO NPs and a specific surface area of 72 $m^2$ $g^{-1}$ was achieved. The adsorption capacity of Congo red has been studied. The PS-MgO (0.05 g $L^{-1}$) was added to Congo red solutions (200 mg $L^{-1}$), removed almost 80% within 10 min and completely adsorbed within 120 min.

Furthermore, the importance of MgO NPs in enabling it to adsorb various divalent metallic species is further evidenced.[134] Flower-shaped MgO NPs were obtained using biocompatible acacia gum, as shown in Fig. 11c. The MgO NPs were synthesized by a chemical precipitation method. Then, the MgO NPs were used as adsorbents for the abatement of divalent metallic ions [Co(II), Cd(II), Zn(II), Cu(II), Mn(II), Pb(II) and Ni(II)] from wastewater, and the efficiency of the absorption is relatively high.

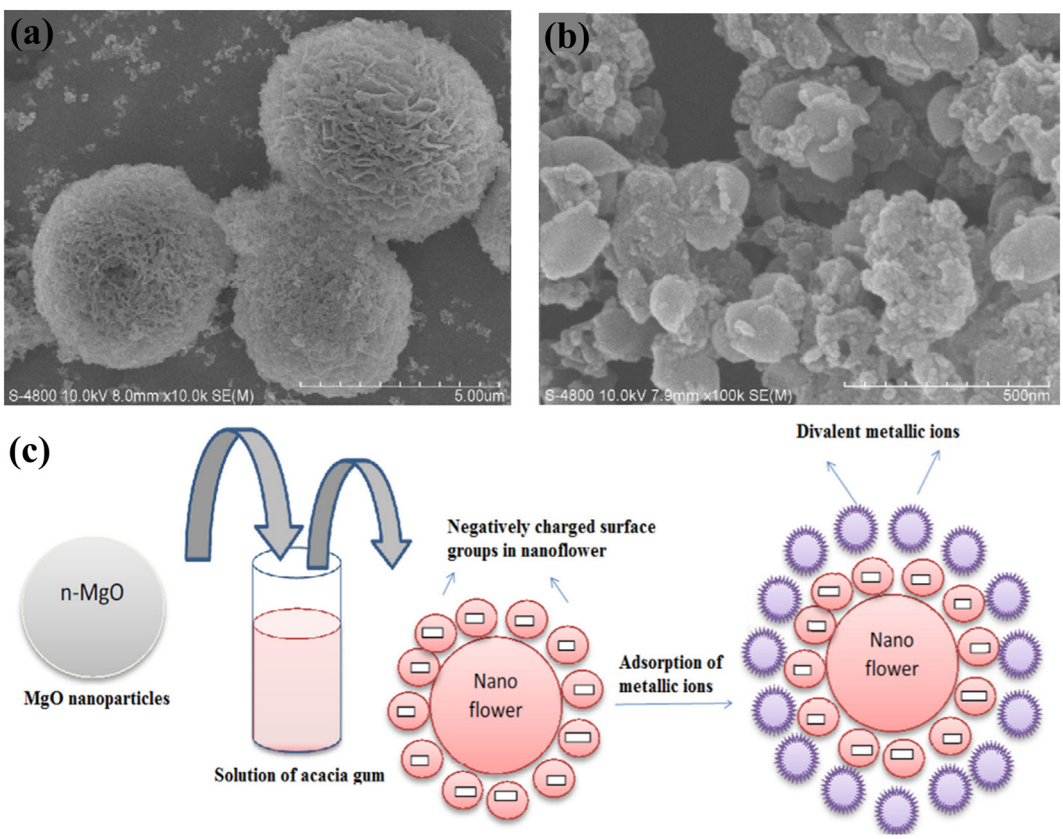


**Fig. 11** SEM images of MgO NPs samples. (a) Low magnification SEM image, (b) high magnification SEM image.[146] (c) Mechanism of flower-shaped MgO NPs synthesis and adsorption.[134] 

The production rate of phosphorous wastes has grown rapidly in recent decades due to the manufacture of a large number of pesticides, artificial fertilizers, and detergents. In relation to these serious environmental problems, research efforts have been carried out to seek effective methods of removing phosphate ions from areas at risk.[145–147] Zhou *et al.*[146] prepared mesoporous MgO NPs by precipitation and calcination using sodium poly(4-styrenesulfonate) (PSS) as a structure-directing agent. Then, the adsorption of phosphate ions on synthesized MgO NPs was studied. The pore structure and SEM analysis showed that the MgO microspheres were composed of at least three levels of hierarchical porous organization, including small mesopores (2–5 nm), large mesopores (10–50 nm) and macropores (50–250 nm). The surface and textural morphology of MgO NPs were observed by SEM (Fig. 11a and b). It shows that MgO NPs are mainly composed of many interleaving petal-like nanoflakes growing in all directions, and consequently constitute interconnected porous networks. Langmuir's equation was used to determine the adsorption capacity of the MgO NPs in pure water and after adding 1 g $L^{-1}$ PSS. The results show that the nanocomposite has greater adsorption capacity for phosphorus, with adsorption of 75.13 mg $g^{-1}$.

In recent years, researchers have developed new synthesis methods to produce materials with better physicochemical and practical properties.[135,148] However, the challenges it faces cannot be ignored, such as high cost and low preparation efficiency.[140] Some synthetic approaches require complex post-processing steps, reducing the overall preparation efficiency.[149] Other synthetic methods use toxic chemicals, which may pollute the environment.[139] A very important and innovative step is the combination of MgO NPs with widely used biopolymers, which include cellulose and its derivatives,[117] chitin,[150] polyvinyl alcohol (PVA),[151] and other materials. This will give multifunctional hybrid materials for specific applications.

### 3.3 Zirconium dioxide nanoparticles

Zirconium dioxide ($ZrO_2$) is a non-hazardous, commercially economical, and sustainable metal oxide that possesses diversified applications, such as reinforcement of structures, antimicrobial agent, adsorption, and photodegradation.[17,113,152–155] Such promising utilizations make it an ideal nanomaterial, and promote the research progress in the synthesis of $ZrO_2$ nanoparticles ($ZrO_2$ NPs). Methods for the synthesis of $ZrO_2$ NPs have been investigated in some studies.[156,157] However, the conventional methods used require toxic solvents, producing residues that are harmful to health and the environment. Thus, the green synthesis in the production of $ZrO_2$ NPs is promising.[17,158]

Tetracycline (TC) is one of the antibiotic drugs that can be mainly found in hospitals, rivers, and wastewater. Some studies have reported that it can promote the evolution of antibiotic resistance genes.[159,160] The $ZrO_2$ NPs were synthesized using *Euclea natalensis* root extract, which exhibits a high adsorption capacity for TC.[17] The $ZrO_2$ NPs were tetragonal phase with a small particle size (5.90–8.54 nm). Factors of extract concentration (extract *C*) and calcination temperature (calcination *T*) are labeled from −1 to 1, which ranges from 50 to 100 g $L^{-1}$ and 550 to 650 °C respectively, as shown in Fig. 12a. The $ZrO_2$ NPs obtained with extract concentration of 50 g $L^{-1}$ and calcination temperature of 550 °C should present the optimal performance, and it exhibits the best adsorptive capacity of 30.45 mg $g^{-1}$ for TC. To improve adsorption capacity, Debnath *et al.*[161] synthesized the $ZrO_2$ NPs in the green method by the bacterial community. They optimized the operating parameters for TC adsorption, such as pH and contact time, and the best adsorption capacity reached the very promising removal value of 526.32 mg $g^{-1}$, and solution pH is 6.0. It further declares that the interaction is a chemisorption phenomenon, as shown in Fig. 12b. As the concentration of $ZrO_2$ NPs increases, the adsorption capacity of TC is enhanced, which is due to the availability of more active sites on the surface of the NPs.[162]

$ZrO_2$ NPs can effectively remove textile dyes such as MB and MO by means of absorption and photodegradation. The $ZrO_2$ NPs biosynthesized from the pericarp extract of *Sapindus mukorossi* exhibit the best absorption capacity of removing 94% MB for 300 min.[155] Another research shows that both MB and MO dyes could be sufficiently degraded by green $ZrO_2$ NPs biosynthesized from the *Ficus benghalensis* leaves under ultra-

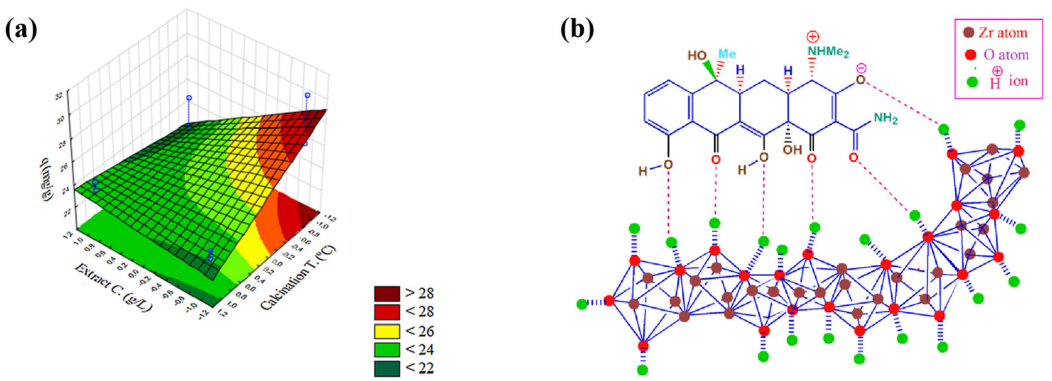


Fig. 12 (a) The response surface with respect to the TC adsorption that relates two factors (the extract concentration and calcination temperature).[17] Copyright © 2019 Elsevier B.V. All rights reserved. (b) The schematic diagram for probable interaction between TC molecules and $ZrO_2$ NPs.[161] Copyright © 2020 Elsevier Ltd. All rights reserved.

violet (UV) light irradiation.[163] It is reported that photodegradation of MB and MO up to 91% and 69% within 240 min, respectively. Similar to other photocatalysts, the electrons ($e^-$) are generated in the conduction band of $ZrO_2$, and interact with the oxygen molecules absorbed on $ZrO_2$ to produce $-O_2^-$. The holes generated in the valence band of $ZrO_2$ act as an oxidizing agent, leading to the formation of –OH. Dyes absorbed on $ZrO_2$ are degraded by –OH and $-O_2^-$.

Due to the excellent properties of green $ZrO_2$ NPs, it is expected to make a significant contribution to the development of novel environmental remediation methods.[164] Ultimately, the combination of dopants with green $ZrO_2$ NPs could expand many promising applications.[152] However, it is generally difficult to control the interactions of green extract with the dopants during the process of preparing $ZrO_2$ NPs based nanomaterials.[165,166] To better understand the formation mechanism and application of green $ZrO_2$ NPs, further research about the overall interactions between $ZrO_2$ NPs and the environment is needed.

### 3.4 Iron oxide nanoparticles

Iron oxide nanoparticles ($Fe_3O_4$ NPs) are composed of iron and oxygen atoms and possess an interesting crystalline structure. The $Fe_3O_4$ NPs are used in wastewater treatment and environmental remediation due to their magnetic properties.[167–171] $Fe_3O_4$ NPs find applications in wastewater treatment and environmental remediation due to their magnetic properties, which facilitate their efficient and reusable removal from water using magnetic fields after adsorption or catalytic degradation of impurities.[172]

For the removal of MB and cresol red (CR), superparamagnetic core–shell NPs with $Fe_3O_4$ NPs as the core and carbon (C) as the shell were synthesized.[168] The average size of NPs was 250 nm. Fig. 13a shows that the adsorption of MB and CR increases with the increase of treating time, then gradually tends to stabilize, and attains about 90% of adsorption capacity at equilibrium within 2.5 h. After the adsorption, these NPs can be easily separated by an external magnet. As shown in Fig. 13b, the adsorption capacity of MB is higher than CR at all concentration ranges. The maximum adsorption capacities for MB and CR of 44.38 mg $g^{-1}$ and 11.22 mg $g^{-1}$, respectively.

It is reported that the $Fe_3O_4$ NPs were treated with gum arabic, and they were used for the removal of Cu(II).[169] The chemical adsorption is efficient and fast, and the equilibrium was achieved within 2 min. The maximum adsorption capacity was 38.5 mg $g^{-1}$ for the $Fe_3O_4$ NPs. In addition, the copper ions could be desorbed from $Fe_3O_4$ NPs by using an acid solution, and the $Fe_3O_4$ NPs exhibited good reusability.

On the other hand, the $Fe_3O_4$ NPs were synthesized using *Simmondsia chinensis* (jojoba) defatted meal extract.[170] Then the $Fe_3O_4$ NPs were impregnated onto polyurethane foam (PUF) and made into tea infusion bags. The calculated average crystallite size of the NPs is 51.48 nm. The $Fe_3O_4$ NPs-PUF displayed a water defluorination capacity of 34.48 mg $g^{-1}$ of fluoride (F). The effects of different parameters (pH, contact time, size of PUF, and initial F concentration) were verified by experiments. The percentage of F removal increased with increasing pH up to 5, while it decreased in the pH range of 5.0–9.0. The adsorption enhances with time, and an equilibrium state is attained after a contact time of 80 min.

While the $Fe_3O_4$ NPs offer many advantages, further research is essential to determine their biocompatibility and long-term environmental impact.[119] The research needs to be continued to improve production processes and surface modifications, which exploit their potential in different industries, from healthcare to environmental sustainability.

### 3.5 Titanium dioxide nanoparticles

Titanium dioxide nanoparticles ($TiO_2$ NPs) exhibit unique characteristics, such as excellent photocatalytic performance,[173] efficient adsorption capacity of heavy metals and fluoride,[18] and innovative materials.[174] There are many strategies with fine control of its morphology.[175] $TiO_2$ NPs of different size and shape, including hollow spherical $TiO_2$ have all been synthesized,[176,177] and have exhibited favorable properties in environmental applications.[18,178–182]

The $TiO_2$ NPs can remove pollutants in wastewater by adsorption. The $TiO_2$ NPs with a particle size range of 19.29–26.72 nm were synthesized by sol–gel method and calcined at a temperature of 400 °C.[18] Their removal effects on Cd(II) in wastewater were studied. The adsorption rate of Cd(II) was very fast in the first 30 min, then the adsorption equili-

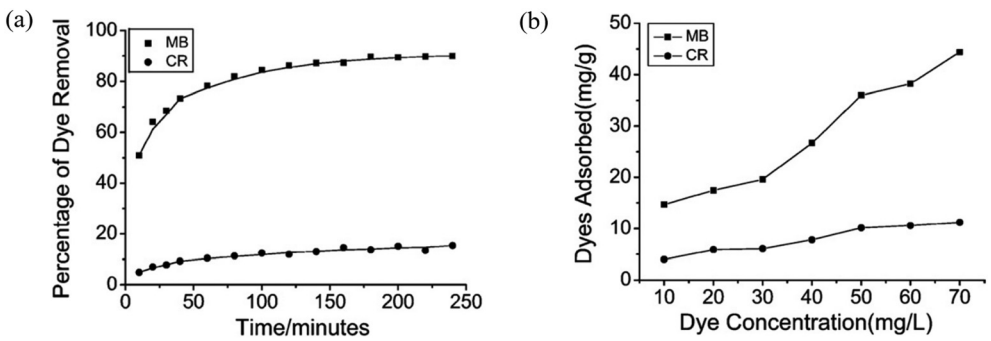


Fig. 13 The effect of experimental parameters on the adsorption of dyes (MB and CR) to $Fe_3O_4$/C core–shell NPs. (a) Contact time, (b) different dye equilibrium concentrations.[168] Copyright © Elsevier B.V. All rights reserved.

brium was reached. The maximum adsorption capacity was 29.28 mg $g^{-1}$ at pH = 6 after a contact time of 180 min.

S. P. Suriyaraj *et al.*[183] investigated the capacity of fluoride ions ($F^-$) onto various phases of $TiO_2$ NPs synthesized by a microbial synthesis method. The $TiO_2$ NPs were transformed into various phases, such as anatase, anatase mixed rutile, and rutile, and they were characterized using a high-resolution transmission electron microscope (HR-TEM), as shown in Fig. 14a–d. The anatase phase of $TiO_2$ NPs showed maximum $F^-$ removal followed by native. The adsorption of $F^-$ depended on the phase of $TiO_2$ NPs obtained after calcinations. The different phases of $TiO_2$ NPs showed the maximum $F^-$ removal of more than 90% at pH range of 2–4. It is revealed that microbially synthesized $TiO_2$ NPs could be a viable, eco-friendly, and green approach for fluoride removal from drinking water.

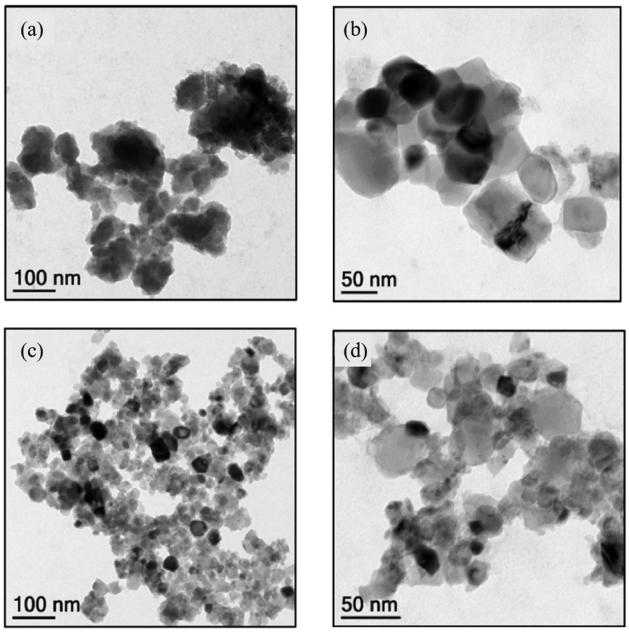


**Fig. 14** HR-TEM images of biosynthesized NPs. (a) Native $TiO_2$ NPs; (b) anatase NPs; (c) anatase and rutile NPs mix; (d) rutile NPs.[183] Copyright © 2014 Elsevier Ltd. All rights reserved.

Semiconductors, for example, hollow spherical $TiO_2$ NPs commonly used in these photocatalytic applications, are involved in similar complex processes.[180] When exposed to UV or visible light, the $TiO_2$ NPs generate electron–hole pairs, as shown in Fig. 15c. The photogenerated electrons and holes migrate to the surface and participate in reduction and oxidation reactions, respectively.[178] It has been widely investigated the effect of $TiO_2$ NPs morphology on its photoactivity.[177,184,185] Hollow spherical $TiO_2$ NPs show high activity in photocatalysis applications because of their controllable shell thickness, high surface area, and easy penetration into the reactant.[177]

The hollow spherical $TiO_2$ NPs were synthesized by assembling $SiO_2/TiO_2$ core–shell composites, with subsequent alkaline etching to remove the $SiO_2$ core, acid treatment, and then calcined at high temperature.[185] It provides the structure of optimized hollow $TiO_2$ shells for efficient photocatalysts that outperform commercial P25-$TiO_2$ in the photocatalytic decomposition of organic dye molecules.

Furthermore, the hollow spherical $TiO_2$ NPs loaded with plasmonic materials (Ag and Au NPs) and doped with nitrogen

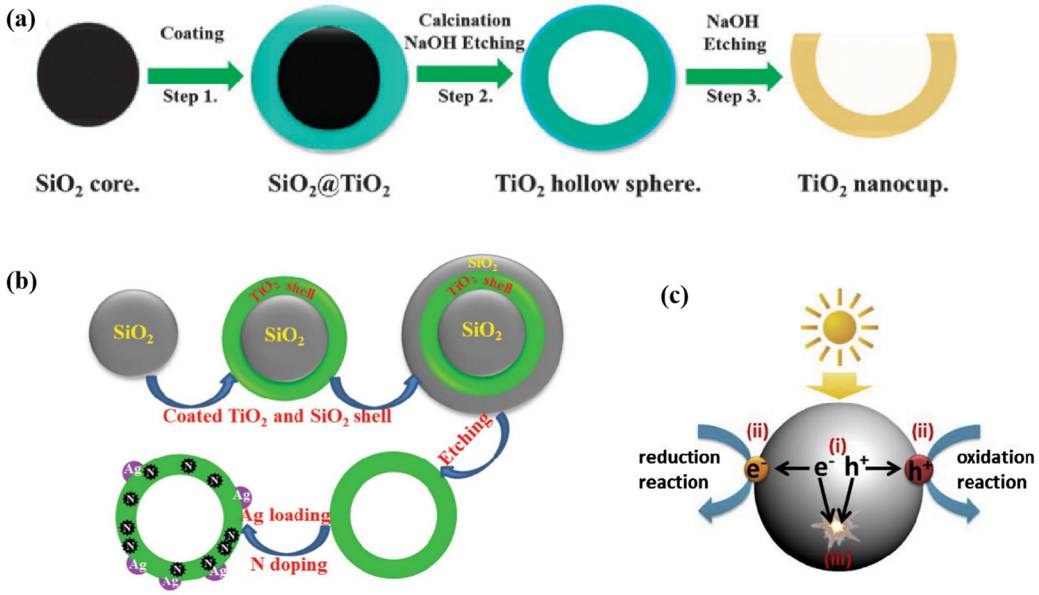


**Fig. 15** Synthetic process of different types of $TiO_2$ hollow spheres. (a) $TiO_2$ nanocups.[181] (b) Ag–N/$TiO_2$ hollow spheres.[182] (c) Schematic illustration of processes involved in semiconductor photocatalysis.[180] Copyright © 2015 Chinese Society of Particuology and Institute of Process Engineering, Chinese Academy of Sciences. Published by Elsevier B.V. All rights reserved. Reproduced from ref. 181 with permission from the Royal Society of Chemistry. Copyright © Reproduced from ref. 182 with permission from the Royal Society of Chemistry.

Table 4 A systematic comparison of the merits and drawbacks of noble metal, transition metal, and metal oxide nanoparticles in environmental remediation applications

| Type of NPs | Advantages | Disadvantages |
|---|---|---|
| Noble metal NPs | Unique optical and electronic properties; exceptional photocatalytic degradation efficiency; biocompatibility | High cost and limited abundance |
| Transition metal NPs | Superior catalytic and redox activity; low-cost and abundance; versatile environmental applications | Toxicity and limited removal capacity of biosynthesized NPs |
| Metal oxide NPs | Exceptional photocatalytic performance; multifunctional environmental applications; chemical stability | Toxicity and environmental risks; high energy and cost barriers |

were developed.[181,182] The well-defined anatase $TiO_2$ hollow sphere, as an intermediate product, was synthesized for further etching treatment using NaOH, as shown in Fig. 15a. Then, the cup-like $TiO_2$ NPs were produced. The cup-like $TiO_2$ NPs decorated with well-dispersed Au NPs exhibit relatively high conversion efficiency of solar energy to photodegradation of organic dyes. Moreover, the $TiO_2$ NPs modified *via* nitrogen doping and silver loading (Ag–N/$TiO_2$) exhibit higher activity for the degradation of MB and MO under visible light irradiation than pure $TiO_2$ hollow sphere, as is shown in Fig. 15b. These modified nanocomposites enhanced the absorption of $TiO_2$ hollow spheres and thus exhibited improved dye degradation activity under visible light irradiation.[186]

In environmental applications, $TiO_2$ NPs are expected to play an increasingly critical role in large-scale pollutant degradation and water purification. Future developments will likely focus on improving their photocatalytic efficiency in different environmental conditions, such as varying light irradiation and catalytic reaction parameters, thus expanding their usability in real-world scenarios.

Metal oxide NPs are synthesized and applied in a very promising area of nanotechnology and materials science.[187] Metal oxide NPs demonstrate remarkable capability in removing diverse contaminants (*e.g.*, phosphate, tetracycline, Congo red, methylene blue, Cu(II)) through adsorption mechanisms. Biosynthesis approaches have attracted significant research attention due to their significant advantages in reducing toxicity during fabrication. For instance, biologically synthesized $ZrO_2$ NPs, after process optimization, exhibited enhanced tetracycline degradation efficiency, increasing from 30.45 mg $g^{-1}$ to 526.32 mg $g^{-1}$. Furthermore, it serves as an effective photocatalyst for dye degradation.[188] Researchers have developed innovative morphological designs, including cup-like and hollow spherical $TiO_2$ NPs. These engineered morphologies significantly increase specific surface area, thereby improving both adsorption capacity and removal efficiency.

The following table presents a comparative comparison of the advantages and disadvantages of different nanoparticles (Table 4).

## 4. Conclusions and outlooks

In summary, metal and metal oxide NPs have great potential in combating pollution and promoting environmental sustainability. Their exceptional properties, including high surface area, degradation, and adsorption capacities, make them potent tools for degrading and removing chemical species from water and the atmosphere. By photocatalytic, degradation, and adsorption, these NPs play a crucial role in safeguarding ecosystems and mitigating the harmful environmental impacts of industrial activities. Especially in textiles and dyes, the application of metal and metal oxide NPs has achieved remarkable results in wastewater treatment. After the treatment, the dyes, heavy metals, and toxicity are significantly reduced, and the water is less harmful to living organisms. The review systematically analyzes the size and morphological characteristics of NPs synthesized *via* different methods, offering critical insights for researchers in nanoparticle fabrication.

For future research, emphasis should be placed on: (i) optimized biosynthesis protocols using diverse biological sources (plants, fungi, bacteria) and solvent systems (aqueous, ionic liquids),[189] (ii) morphology-controlled synthesis (octahedral, spherical, *etc.*) for enhanced performance,[190] and (iii) scalable production with rigorous toxicity assessments.[191] By leveraging metal and metal oxide NPs' unique properties, this approach aims to explore environmentally sustainable nanomaterials with superior contaminant removal efficiency and broad applicability. Key challenges, including agglomeration, toxicity, and cost, must be addressed through innovative solutions to minimize secondary pollution and enable widespread environmental applications.

## Data availability

Data availability is not applicable to this review article as no new data were created or analyzed in this study.

## Conflicts of interest

There are no conflicts to declare.

## Acknowledgements

This research is supported by the startup project from Hangzhou Normal University.

## References

1 A. Roy, H. C. A. Murthy, H. M. Ahmed, M. N. Islam and R. Prasad, *J. Renewable Mater.*, 2022, **10**, 1911–1930.
2 C. S. P. Coll, C. Pabón-Reyes, J. M. Meichtry and M. I. Litter, *Environ. Toxicol. Pharmacol.*, 2018, **60**, 138–145.
3 B. Xue, Q. Yang, K. Xia, Z. Li, G. Y. Chen, D. Zhang and X. Zhou, *Engineering*, 2023, **27**, 199–208.
4 P. Somu and S. Paul, *J. Chem. Technol. Biotechnol.*, 2018, **93**, 2962–2976.
5 P. C. Nagajyothi, S. V. P. Vattikuti, K. C. Devarayapalli, K. Yoo, J. Shim and T. V. M. Sreekanth, *Crit. Rev. Environ. Sci. Technol.*, 2020, **50**, 2617–2723.
6 K. M. Lee, C. W. Lai, K. S. Ngai and J. C. Juan, *Water Res.*, 2016, **88**, 428–448.
7 Y. Xia, P. Yang, Y. Sun, Y. Wu, B. Mayers, B. Gates, Y. Yin, F. Kim and H. Yan, *Adv. Mater.*, 2003, **15**, 353–389.
8 M. B. Gawande, A. Goswami, F. X. Felpin, T. Asefa, X. Huang, R. Silva, X. Zou, R. Zboril and R. S. Varma, *Chem. Rev.*, 2016, **116**, 3722–3811.
9 S. Cong, Y. Yuan, Z. Chen, J. Hou, M. Yang, Y. Su, Y. Zhang, L. Li, Q. Li, F. Geng and Z. Zhao, *Nat. Commun.*, 2015, **6**, 7800.
10 J. Cao, T. Sun and K. T. V. Grattan, *Sens. Actuators, B*, 2014, **195**, 332–351.
11 J. Fabrega, S. N. Luoma, C. R. Tyler, T. S. Galloway and J. R. Lead, *Environ. Int.*, 2011, **37**, 517–531.
12 L. Rassaei, F. Marken, M. Sillanpää, M. Amiri, C. M. Cirtiu and M. Sillanpää, *TrAC, Trends Anal. Chem.*, 2011, **30**, 1704–1715.
13 S. Marimuthu, A. J. Antonisamy, S. Malayandi, K. Rajendran, P.-C. Tsai, A. Pugazhendhi and V. K. Ponnusamy, *J. Photochem. Photobiol., B*, 2020, **205**, 111823.
14 T. Ahmed, M. Noman, M. Shahid, M. B. K. Niazi, S. Hussain, N. Manzoor, X. Wang and B. Li, *Environ. Res.*, 2020, **191**, 110142.
15 Z. Fang, X. Qiu, J. Chen and X. Qiu, *J. Hazard. Mater.*, 2011, **185**, 958–969.
16 B. Siripireddy and B. K. Mandal, *Adv. Powder Technol.*, 2017, **28**, 785–797.
17 A. F. V. da Silva, A. P. Fagundes, D. L. P. Macuvele, E. F. U. de Carvalho, M. Durazzo, N. Padoin, C. Soares and H. G. Riella, *Colloids Surf., A*, 2019, **583**, 123915.
18 S. E. A. S. El-Deen and F.-S. Zhang, *J. Exp. Nanosci.*, 2015, **11**, 239–258.
19 X. Pan, F. Kong and M. Xing, *Res. Chem. Intermed.*, 2022, **48**, 2837–2855.
20 P. G. Jamkhande, N. W. Ghule, A. H. Bamer and M. G. Kalaskar, *J. Drug Delivery Sci. Technol.*, 2019, **53**, 101174.
21 X. Pan, J. Ji, N. Zhang and M. Xing, *Chin. Chem. Lett.*, 2020, **31**, 1462–1473.
22 M. Azharuddin, G. H. Zhu, D. Das, E. Ozgur, L. Uzun, A. P. F. Turner and H. K. Patra, *Chem. Commun.*, 2019, **55**, 6964–6996.
23 H. Liu, T. Lian, Y. Liu, Y. Hong, D. Sun and Q. Li, *Ind. Eng. Chem. Res.*, 2017, **56**, 5262–5270.
24 P. Dauthal and M. Mukhopadhyay, *Ind. Eng. Chem. Res.*, 2016, **55**, 9557–9577.
25 F. Okafor, A. Janen, T. Kukhtareva, V. Edwards and M. Curley, *Int. J. Environ. Res. Public Health*, 2013, **10**, 5221–5238.
26 L. A. Austin, M. A. Mackey, E. C. Dreaden and M. A. El-Sayed, *Arch. Toxicol.*, 2014, **88**, 1391–1417.
27 P. K. Jain, X. Huang, I. H. El-Sayed and M. A. El-Sayed, *Plasmonics*, 2007, **2**, 107–118.
28 K. M. M. Abou El-Nour, A. a. Eftaiha, A. Al-Warthan and R. A. A. Ammar, *Arabian J. Chem.*, 2010, **3**, 135–140.
29 P. Jain and T. Pradeep, *Biotechnol. Bioeng.*, 2005, **90**, 59–63.
30 X. Bai, Y. Gao, H.-g. Liu and L. Zheng, *J. Phys. Chem. C*, 2009, **113**, 17730–17736.
31 Z.-J. Jiang, C.-Y. Liu and L.-W. Sun, *J. Phys. Chem. B*, 2005, **109**, 1730–1735.
32 C. Zhang, Z. Hu and B. Deng, *Water Res.*, 2016, **88**, 403–427.
33 E. McGillicuddy, I. Murray, S. Kavanagh, L. Morrison, A. Fogarty, M. Cormican, P. Dockery, M. Prendergast, N. Rowan and D. Morris, *Sci. Total Environ.*, 2017, **575**, 231–246.
34 A. M. Atta, Y. M. Moustafa, H. A. Al-Lohedan, A. O. Ezzat and A. I. Hashem, *ACS Omega*, 2020, **5**, 2829–2842.
35 S. J. Klaine, P. J. J. Alvarez, G. E. Batley, T. F. Fernandes, R. D. Handy, D. Y. Lyon, S. Mahendra, M. J. McLaughlin and J. R. Lead, *Environ. Toxicol. Chem.*, 2008, **27**, 1825–1851.
36 S. Niakan, M. Niakan, S. Hesaraki, M. R. Nejadmoghaddam, M. Moradi, M. Hanafiabdar, R. Allamezadeh and M. Sabouri, *Jundishapur J. Microbiol.*, 2013, **6**, e8341.
37 K. J. Kim, W. S. Sung, S. K. Moon, J. S. Choi, J. G. Kim and D. G. Lee, *J. Microbiol. Biotechnol.*, 2008, **18**, 1482–1484.
38 K. Y. Yoon, J. H. Byeon, C. W. Park and J. Hwang, *Environ. Sci. Technol.*, 2008, **42**, 1251–1255.
39 K. V. Alex, P. T. Pavai, R. Rugmini, M. S. Prasad, K. Kamakshi and K. C. Sekhar, *ACS Omega*, 2020, **5**, 13123–13129.
40 N. Soltani, E. Saion, M. Z. Hussein, M. Erfani, A. Abedini, G. Bahmanrokh, M. Navasery and P. Vaziri, *Int. J. Mol. Sci.*, 2012, **13**, 12242–12258.
41 P. Mukherjee, A. Ahmad, D. Mandal, S. Senapati, S. R. Sainkar, M. I. Khan, R. Parishcha, P. V. Ajaykumar, M. Alam, R. Kumar and M. Sastry, *Nano Lett.*, 2001, **1**, 515–519.
42 S. Iravani, *Green Chem.*, 2011, **13**, 2638.
43 M. Kowshik, S. Ashtaputre, S. Kharrazi, W. Vogel, J. Urban, S. K. Kulkarni and K. M. Paknikar, *Nanotechnology*, 2003, **14**, 95.
44 M. Ghaedi, S. Heidarpour, S. N. Kokhdan, R. Sahraie, A. Daneshfar and B. Brazesh, *Powder Technol.*, 2012, **228**, 18–25.

 

45 S. K. Das, M. M. R. Khan, T. Parandhaman, F. Laffir, A. K. Guha, G. Sekaran and A. B. Mandal, *Nanoscale*, 2013, **5**, 5549.
46 G. Liao, Q. Li, W. Zhao, Q. Pang, H. Gao and Z. Xu, *Appl. Catal., A*, 2018, **549**, 102–111.
47 B. Le Ouay and F. Stellacci, *Nano Today*, 2015, **10**, 339–354.
48 Z. Xiong, L. L. Zhang, J. Ma and X. S. Zhao, *Chem. Commun.*, 2010, **46**, 6099–6101.
49 T. Momić, T. L. Pašti, U. Bogdanović, V. Vodnik, A. Mraković, Z. Rakočević, V. B. Pavlović and V. Vasić, *J. Nanomater.*, 2016, **2016**, 1–11.
50 P. Ghosh, G. Han, M. De, C. Kim and V. Rotello, *Adv. Drug Delivery Rev.*, 2008, **60**, 1307–1315.
51 N. Sarfraz and I. Khan, *Chem. – Asian J.*, 2021, **16**, 720–742.
52 C. Wang and D. Astruc, *Chem. Soc. Rev.*, 2014, **43**, 7188–7216.
53 J. Wang, S. Fan, Y. Xia, C. Yang and S. Komarneni, *J. Hazard. Mater.*, 2020, **381**, 120919.
54 J. J. Zhang, L. Mou and X. Y. Jiang, *Chem. Sci.*, 2020, **11**, 923–936.
55 S. Ghosh, S. Roy, J. Naskar and R. K. Kole, *Sci. Rep.*, 2020, **10**, 277.
56 R. K. Singh, S. S. Behera, K. R. Singh, S. Mishra, B. Panigrahi, T. R. Sahoo, P. K. Parhi and D. Mandal, *J. Photochem. Photobiol., A*, 2020, **400**, 112704.
57 P. K. Jain, K. S. Lee, I. H. El-Sayed and M. A. El-Sayed, *J. Phys. Chem. B*, 2006, **110**, 7238–7248.
58 S. Mondal, M. E. De Anda Reyes and U. Pal, *RSC Adv.*, 2017, **7**, 8633–8645.
59 J. Herdan, R. Feeney, S. P. Kounaves, A. F. Flannery, C. W. Storment, G. T. A. Kovacs and R. B. Darling, *Environ. Sci. Technol.*, 1998, **32**, 131–136.
60 Q. Lu, L. Zhu, S. Han, Y. Hou and W. Cao, *Phys. Chem. Chem. Phys.*, 2019, **21**, 18753–18757.
61 S. Y. Lee, D. Kang, S. Jeong, H. T. Do and J. H. Kim, *ACS Omega*, 2020, **5**, 4233–4241.
62 M. Sengan, R. K. Kamlekar and A. Veerappan, *Spectrochim. Acta, Part A*, 2020, **239**, 118485.
63 C. Hano and B. H. Abbasi, *Biomolecules*, 2021, **12**, 31.
64 T. Xiao, J. Huang, D. Wang, T. Meng and X. Yang, *Talanta*, 2020, **206**, 120210.
65 H. Yang, L. Shang, Q. Zhang, R. Shi, G. I. N. Waterhouse, L. Gu and T. Zhang, *Nat. Commun.*, 2019, **10**, 4585.
66 Y. Zhao, *J. Mater. Res. Technol.*, 2022, **21**, 546–560.
67 K. Qi, X. Xing, A. Zada, M. Li, Q. Wang, S.-y. Liu, H. Lin and G. Wang, *Ceram. Int.*, 2020, **46**, 1494–1502.
68 A. Nandagudi, S. H. Nagarajarao, M. S. Santosh, B. M. Basavaraja, S. J. Malode, R. J. Mascarenhas and N. P. Shetti, *Mater. Today Sustainability*, 2022, **19**, 100214.
69 Y. He, Z. Yin, Z. Wang, H. Wang, W. Xiong, B. Song, H. Qin, P. Xu and G. Zeng, *J. Mater. Chem. A*, 2022, **10**, 9788–9820.
70 N. A. C. Lah, *Renewable Sustainable Energy Rev.*, 2021, **145**, 111103.
71 A. Burton, *Environ. Health Perspect.*, 2009, **117**, A552–A552.
72 P. Sangaiya and R. Jayaprakash, *J. Supercond. Novel Magn.*, 2018, **31**, 3397–3413.
73 C. D. Raman and S. Kanmani, *Environ. Prog. Sustain. Energy*, 2018, **38**, S366–S376.
74 M. Iv, N. Telischak, D. Feng, S. J. Holdsworth, K. W. Yeom and H. E. Daldrup-Link, *Nanomedicine*, 2015, **10**, 993–1018.
75 H. Wu and H. Zhang, *Foods*, 2022, **11**, 1382.
76 R. Mo, *Coatings*, 2022, **12**, 809.
77 K. S. Ahmad, M. Nawaz and S. B. Jaffri, *Int. J. Environ. Anal. Chem.*, 2020, **102**, 7700–7719.
78 C. P. Devatha, A. K. Thalla and S. Y. Katte, *J. Cleaner Prod.*, 2016, **139**, 1425–1435.
79 F. Fu, D. D. Dionysiou and H. Liu, *J. Hazard. Mater.*, 2014, **267**, 194–205.
80 P.-A. Yang, Y. Huang, R. Li, X. Huang, H. Ruan, M. Shou, W. Li, Y. Zhang, N. Li and L. Dong, *Chem. Eng. J.*, 2022, **430**, 132878.
81 S. M. Ponder, J. G. Darab and T. E. Mallouk, *Environ. Sci. Technol.*, 2000, **34**, 2564–2569.
82 Y. Kuang, Q. Wang, Z. Chen, M. Megharaj and R. Naidu, *J. Colloid Interface Sci.*, 2013, **410**, 67–73.
83 Y. Wei, Z. Fang, L. Zheng and E. P. Tsang, *Appl. Surf. Sci.*, 2017, **399**, 322–329.
84 M. Harshiny, C. N. Iswarya and M. Matheswaran, *Powder Technol.*, 2015, **286**, 744–749.
85 X. Zhao, W. Liu, Z. Cai, B. Han, T. Qian and D. Zhao, *Water Res.*, 2016, **100**, 245–266.
86 C. Fajardo, M. Gil-Díaz, G. Costa, J. Alonso, A. M. Guerrero, M. Nande, M. C. Lobo and M. Martín, *Sci. Total Environ.*, 2015, **535**, 79–84.
87 R. W. Gillham and S. F. O'Hannesin, *Groundwater*, 2005, **32**, 958–967.
88 S. R. Kanel, B. Manning, L. Charlet and H. Choi, *Environ. Sci. Technol.*, 2005, **39**, 1291–1298.
89 B. D. Yirsaw, M. Megharaj, Z. Chen and R. Naidu, *J. Environ. Sci.*, 2016, **44**, 88–98.
90 C. Macé, S. Desrocher, F. Gheorghiu, A. Kane, M. Pupeza, M. Cernik, P. Kvapil, R. Venkatakrishnan and W. x. Zhang, *Rem. J.*, 2006, **16**, 23–33.
91 X. Qiu, Z. Fang, X. Yan, W. Cheng and K. Lin, *Chem. Eng. J.*, 2013, **220**, 61–66.
92 Y. Mu, F. Jia, Z. Ai and L. Zhang, *Environ. Sci.: Nano*, 2017, **4**, 27–45.
93 F. Fu, J. Ma, L. Xie, B. Tang, W. Han and S. Lin, *J. Environ. Manage.*, 2013, **128**, 822–827.
94 A. Iqbal, K. Iqbal, B. Li, D. Gong and W. Qin, *J. Nanosci. Nanotechnol.*, 2017, **17**, 4386–4409.
95 J. Zhang, J. Liu, Q. Peng, X. Wang and Y. Li, *Chem. Mater.*, 2006, **18**, 867–871.
96 H. G. Na, H. Y. Cho, Y. J. Kwon, S. Y. Kang, C. Lee, T. K. Jung, H.-S. Lee and H. W. Kim, *Thin Solid Films*, 2015, **588**, 11–18.
97 H. A. Alshaikhi, A. M. Asiri, K. A. Alamry, H. M. Marwani, S. Y. Alfifi and S. B. Khan, *Polymers*, 2022, **14**, 4458.

98 W. Fan, A. Wang, L. Wang, X. Jiang, Z. Xue, J. Li and G. Wang, *ACS Appl. Mater. Interfaces*, 2023, **15**, 13600–13608.
99 J. Mondal, A. Biswas, S. Chiba and Y. Zhao, *Sci. Rep.*, 2015, **5**, 8294.
100 L. Chen, Z. Li, Q. Xiao, M. Li, Y. Xu and X. Qiu, *Appl. Catal., A*, 2023, **649**, 118964.
101 K. Mužina, S. Kurajica, P. Guggenberger, M. Duplančić and G. Dražić, *J. Mater. Res.*, 2022, **37**, 1929–1940.
102 J. H. Byeon, K. Y. Yoon, J. H. Park and J. Hwang, *Carbon*, 2007, **45**, 2313–2316.
103 Y.-P. Li, H.-B. Cao, C.-M. Liu and Y. Zhang, *J. Hazard. Mater.*, 2007, **148**, 158–163.
104 H. Wang, Y. Xu, D. Xu, L. Chen, Q. Xiao and X. Qiu, *Ind. Eng. Chem. Res.*, 2022, **61**, 6301–6310.
105 Y. T. Xu, T. Y. Zhang, Z. Li, X. N. Liu, Y. C. Zhu, W. W. Zhao, H. Y. Chen and J. J. Xu, *Electroanalysis*, 2021, **34**, 947–955.
106 Y. Zang, J. Fan, Y. Ju, H. Xue and H. Pang, *Chem. – Eur. J.*, 2018, **24**, 14010–14027.
107 D. Liang, J. Luo, X. Liang, H. Wang, J. Wang and X. Qiu, *Chemosphere*, 2021, **267**, 129218.
108 M. B. Gawande, A. Goswami, F.-X. Felpin, T. Asefa, X. Huang, R. Silva, X. Zou, R. Zboril and R. S. Varma, *Chem. Rev.*, 2016, **116**, 3722–3811.
109 K. Vijayaraghavan and T. Ashokkumar, *J. Environ. Chem. Eng.*, 2017, **5**, 4866–4883.
110 P. Dikshit, J. Kumar, A. Das, S. Sadhu, S. Sharma, S. Singh, P. Gupta and B. Kim, *Catalysts*, 2021, **11**, 902.
111 J. Jeevanandam, Y. S. Chan and M. K. Danquah, *ChemBioEng Rev.*, 2016, **3**, 55–67.
112 D. Ziental, B. Czarczynska-Goslinska, D. T. Mlynarczyk, A. Glowacka-Sobotta, B. Stanisz, T. Goslinski and L. Sobotta, *Nanomaterials*, 2020, **10**, 387.
113 N. S. Hassan and A. A. Jalil, *J. Hazard. Mater.*, 2022, **423**, 126996.
114 M. Shi, X. Min, Y. Ke, Z. Lin, Z. Yang, S. Wang, N. Peng, X. Yan, S. Luo, J. Wu and Y. Wei, *Sci. Total Environ.*, 2021, **752**, 141930.
115 S. Pansambal, R. Oza, S. Borgave, A. Chauhan, P. Bardapurkar, S. Vyas and S. Ghotekar, *Appl. Nanosci.*, 2022, **13**, 6067–6092.
116 S. Azizi, M. M. Shahri and R. Mohamad, *Molecules*, 2017, **22**, 831.
117 K. D. Khalil, A. H. Bashal, M. Khalafalla and A. A. Zaki, *J. Taibah Univ. Sci.*, 2020, **14**, 975–983.
118 S. H. Gebre and M. G. Sendeku, *SN Appl. Sci.*, 2019, **1**, 928.
119 B. S. Rathi, L. S. Ewe, S. Sanjay, S. Sujatha, W. K. Yew, R. Baskaran and S. K. Tiong, *Nanotoxicology*, 2024, **18**, 272–298.
120 S. D. Senol, B. Yalcin, E. Ozugurlu and L. Arda, *Mater. Res. Express*, 2020, **7**, 015079.
121 C. Belver, J. Bedia, A. Gómez-Avilés, M. Peñas-Garzón and J. J. Rodriguez, *Nanoscale Materials in Water Purification*, 2019, vol. 22, pp. 581–651.
122 S. Bettini, R. Pagano, L. Valli and G. Giancane, *Chem. – Asian J.*, 2016, **11**, 1240–1245.
123 M. Saeed, M. Muneer, A. u. Haq and N. Akram, *Environ. Sci. Pollut. Res.*, 2021, **29**, 293–311.
124 L. Jiang, Y. Wang and C. Feng, *Procedia Eng.*, 2012, **45**, 993–997.
125 N. Verma, S. Bhatia and R. K. Bedi, *J. Mater. Sci.: Mater. Electron.*, 2017, **28**, 9788–9797.
126 X. Jin, C. Yu, Y. Li, Y. Qi, L. Yang, G. Zhao and H. Hu, *J. Hazard. Mater.*, 2011, **186**, 1672–1680.
127 Ihsanullah, A. Abbas, A. M. Al-Amer, T. Laoui, M. J. Al-Marri, M. S. Nasser, M. Khraisheh and M. A. Atieh, *Sep. Purif. Technol.*, 2016, **157**, 141–161.
128 I. Y. Goryacheva, *Comprehensive Analytical Chemistry*, 2016, vol. 72, pp. 79–131.
129 K. Y. Kumar, H. B. Muralidhara, Y. A. Nayaka, H. Hanumanthappa, M. S. Veena and S. R. K. Kumar, International Conference on Advanced Nanomaterials & Emerging Engineering Technologies, Chennai, India, 2013, 95–101.
130 D. Suresh, P. C. Nethravathi, Udayabhanu, H. Rajanaika, H. Nagabhushana and S. C. Sharma, *Mater. Sci. Semicond. Process.*, 2015, **31**, 446–454.
131 S. Gentie, A. Belay, R. A. Chandra and Z. Belay, *J. Nanomed. Nanotechnol.*, 2017, **s8**, 004.
132 A. H. Mandal, S. Ghosh, D. Adhurjya, P. Chatterjee, I. Samajdar, D. Mukherjee, K. Dhara, N. C. Saha, G. Piccione, C. R. Multisanti, S. Saha and C. Faggio, *Aquacult. Rep.*, 2024, **36**, 102038.
133 M. Rizwan, S. Ali, M. F. Qayyum, Y. S. Ok, M. Adrees, M. Ibrahim, M. Zia-ur-Rehman, M. Farid and F. Abbas, *J. Hazard. Mater.*, 2017, **322**, 2–16.
134 V. Srivastava, Y. C. Sharma and M. Sillanpää, *Ceram. Int.*, 2015, **41**, 6702–6709.
135 M. I. Khan, M. N. Akhtar, N. Ashraf, J. Najeeb, H. Munir, T. I. Awan, M. B. Tahir and M. R. Kabli, *Appl. Nanosci.*, 2020, **10**, 2351–2364.
136 A. A. Pilarska, Ł. Klapiszewski and T. Jesionowski, *Powder Technol.*, 2017, **319**, 373–407.
137 T. Wang, Y. Xu, Q. Su, R. Yang, L. Wang, B. Liu, S. Shen, G. Jiang, W. Chen and S. Wang, *Mater. Lett.*, 2014, **116**, 332–336.
138 C. Xiong, W. Wang, F. Tan, F. Luo, J. Chen and X. Qiao, *J. Hazard. Mater.*, 2015, **299**, 664–674.
139 T. Pedro, M. María del Puerto, V.-V. Sabino, G.-C. Teresita and J. S. Carlos, *J. Phys. D: Appl. Phys.*, 2003, **36**, R182.
140 M. Y. Nassar, T. Y. Mohamed, I. S. Ahmed and I. Samir, *J. Mol. Liq.*, 2017, **225**, 730–740.
141 S. Ali, M. A. Farrukh and M. Khaleeq-ur-Rahman, *Korean J. Chem. Eng.*, 2013, **30**, 2100–2107.
142 Y. F. Lai, P. Chaudouët, F. Charlot, I. Matko and C. Dubourdieu, *Appl. Phys. Lett.*, 2009, **94**, 022904.
143 V. Sirota, V. Selemenev, M. Kovaleva, I. Pavlenko, K. Mamunin, V. Dokalov and M. Prozorova, *Phys. Res. Int.*, 2016, **2016**, 1–4.
144 M. Hua, S. Zhang, B. Pan, W. Zhang, L. Lv and Q. Zhang, *J. Hazard. Mater.*, 2012, **211–212**, 317–331.

 

145 R. Li, J. J. Wang, B. Zhou, M. K. Awasthi, A. Ali, Z. Zhang, L. A. Gaston, A. H. Lahori and A. Mahar, *Sci. Total Environ.*, 2016, **559**, 121–129.
146 J. Zhou, S. Yang and J. Yu, *Colloids Surf., A*, 2011, **379**, 102–108.
147 S. Li, Y. Zhang, S. Qiao and J. Zhou, *Chemosphere*, 2022, **307**, 135972.
148 M. Alaei, M. Jalali and A. Rashidi, *Iran. J. Chem. Chem. Eng.*, 2014, **33**, 21–28.
149 A. S. Mukasyan and K. V. Manukyan, *Nanomater. Synth.*, 2019, **4**, 85–120.
150 A. J. Varma, S. V. Deshpande and J. F. Kennedy, *Carbohydr. Polym.*, 2004, **55**, 77–93.
151 S. M. Riyadh, K. D. Khalil and A. H. Bashal, *Catalysts*, 2020, **10**, 100.
152 B. Wang, Y. Guo, Q. Li, C. Xin, Y. Tian, W. Zhang and X. Yu, *Chem. Eng. J.*, 2024, **481**, 148489.
153 J. B. Fathima, A. Pugazhendhi and R. Venis, *Microb. Pathog.*, 2017, **110**, 245–251.
154 R. Chakravarty, R. Shukla, R. Ram, A. K. Tyagi, A. Dash and M. Venkatesh, *Chromatographia*, 2010, **72**, 875–884.
155 A. Alagarsamy, S. Chandrasekaran and A. Manikandan, *J. Mol. Struct.*, 2022, **1247**, 131275.
156 S. Zinatloo-Ajabshir and M. Salavati-Niasari, *J. Mater. Sci.: Mater. Electron.*, 2015, **27**, 3918–3928.
157 C. Liu, T. J. Hajagos, D. Chen, Y. Chen, D. Kishpaugh and Q. Pei, *ACS Appl. Mater. Interfaces*, 2016, **8**, 4795–4802.
158 S. Jadoun, R. Arif, N. K. Jangid and R. K. Meena, *Environ. Chem. Lett.*, 2020, **19**, 355–374.
159 P. Kairigo, E. Ngumba, L.-R. Sundberg, A. Gachanja and T. Tuhkanen, *Sci. Total Environ.*, 2020, **720**, 137580.
160 B. Böger, M. Surek, R. d. O. Vilhena, M. M. Fachi, A. M. Junkert, J. M. M. F. Santos, E. L. Domingos, A. d. F. Cobre, D. R. Momade and R. Pontarolo, *J. Hazard. Mater.*, 2021, **402**, 123448.
161 B. Debnath, M. Majumdar, M. Bhowmik, K. L. Bhowmik, A. Debnath and D. N. Roy, *J. Environ. Manage.*, 2020, **261**, 110235.
162 H. Zhu, T. Chen, J. Liu and D. Li, *RSC Adv.*, 2018, **8**, 2616–2621.
163 H. M. Shinde, T. T. Bhosale, N. L. Gavade, S. B. Babar, R. J. Kamble, B. S. Shirke and K. M. Garadkar, *J. Mater. Sci.: Mater. Electron.*, 2018, **29**, 14055–14064.
164 T. V. Tran, D. T. C. Nguyen, P. S. Kumar, A. T. M. Din, A. A. Jalil and D.-V. N. Vo, *Environ. Chem. Lett.*, 2022, **20**, 1309–1331.
165 N. Al-Zaqri, A. Muthuvel, M. Jothibas, A. Alsalme, F. A. Alharthi and V. Mohana, *Inorg. Chem. Commun.*, 2021, **127**, 108507.
166 W. F. Tharp and L. K. A. Karem, *Moroccan J. Chem.*, 2024, **12**, 643–656.
167 A. Roy, A. Sharma, S. Yadav, L. T. Jule, R. Krishnaraj and W. Aruni, *Bioinorg. Chem. Appl.*, 2021, **2021**, 1764647.
168 Z. Zhang and J. Kong, *J. Hazard. Mater.*, 2011, **193**, 325–329.
169 S. S. Banerjee and D.-H. Chen, *J. Hazard. Mater.*, 2007, **147**, 792–799.
170 S. Kumari and S. Khan, *Sci. Rep.*, 2017, **7**, 8070.
171 J. Feng, X. Hu, P. L. Yue, H. Y. Zhu and G. Q. Lu, *Ind. Eng. Chem. Res.*, 2003, **42**, 2058–2066.
172 S. P. Suriyaraj and R. Selvakumar, *RSC Adv.*, 2016, **6**, 10565–10583.
173 J. C. Colmenares and R. Luque, *Chem. Soc. Rev.*, 2014, **43**, 765–778.
174 M. K. H. M. Nazri and N. Sapawe, *Mater. Today: Proc.*, 2020, **31**, A42–A47.
175 F. E. Osterloh, *Chem. Soc. Rev.*, 2013, **42**, 2294–2320.
176 Y. J. Kim, M. H. Lee, H. J. Kim, G. Lim, Y. S. Choi, N. G. Park, K. Kim and W. I. Lee, *Adv. Mater.*, 2009, **21**, 3668–3673.
177 Y. Jiao, C. Peng, F. Guo, Z. Bao, J. Yang, L. Schmidt-Mende, R. Dunbar, Y. Qin and Z. Deng, *J. Phys. Chem. C*, 2011, **115**, 6405–6409.
178 U. I. Gaya and A. H. Abdullah, *J. Photochem. Photobiol., C*, 2008, **9**, 1–12.
179 S. Dadgostar, F. Tajabadi and N. Taghavinia, *ACS Appl. Mater. Interfaces*, 2012, **4**, 2964–2968.
180 P. Zhang, A. Li and J. L. Gong, *Particuology*, 2015, **22**, 13–23.
181 J. Lu, P. Zhang, A. Li, F. Su, T. Wang, Y. Liu and J. Gong, *Chem. Commun.*, 2013, **49**, 5817.
182 J. Lu, F. Su, Z. Huang, C. Zhang, Y. Liu, X. Ma and J. Gong, *RSC Adv.*, 2013, **3**, 720–724.
183 S. P. Suriyaraj, T. Vijayaraghavan, P. Biji and R. Selvakumar, *J. Environ. Chem. Eng.*, 2014, **2**, 444–454.
184 A. Li, P. Zhang, X. X. Chang, W. T. Cai, T. Wang and J. L. Gong, *Small*, 2015, **11**, 1892–1899.
185 J. B. Joo, I. Lee, M. Dahl, G. D. Moon, F. Zaera and Y. D. Yin, *Adv. Funct. Mater.*, 2013, **23**, 4246–4254.
186 A. Li, P. Zhang, X. Chang, W. Cai, T. Wang and J. Gong, *Small*, 2015, **11**, 1892–1899.
187 M. Z. I. Nizami, V. W. Xu, I. X. Yin, O. Y. Yu and C.-H. Chu, *Nanomaterials*, 2021, 11.
188 C. Zuo, X. Tai, Z. Jiang, M. Liu, J. Jiang, Q. Su and X. Yan, *Molecules*, 2023, 28.
189 A. M. E. Shafey, *Green Process. Synth.*, 2020, **9**, 304–339.
190 D.-M. Radulescu, V.-A. Surdu, A. Ficai, D. Ficai, A.-M. Grumezescu and E. Andronescu, *Int. J. Mol. Sci.*, 2023, **24**, 15397.
191 G. M. Nair, T. Sajini and B. Mathew, *Talanta Open*, 2022, **5**, 100080.